Preprint:

Juusola, M., Takalo, J., Kemppainen, J. et al. (2026) Beyond static perception: Animals, neurons and synapses move to compute efficiently. [Preprint - Preprints.org] (Submitted)

https://doi.org/10.20944/preprints202603.1093.v1

Review

Beyond Static Perception: Animals, Neurons and Synapses Move to Compute Efficiently

Mikko Juusola [*] , Jouni Takalo , Joni Kemppainen , HaDi MaBouDi , Bruce Yi Bu , Shashwat Shukla , Yiyin Zhou , Aurel A. Lazar , Gonzalo de Polavieja

Review

Beyond Static Perception: Animals, Neurons and Synapses Move to Compute Efficiently

Mikko Juusola [1,2,*], **Jouni Takalo** [1,2], **Joni Kemppainen** [1,2], **HaDi MaBouDi** [1,2], **Bruce Yi Bu** [3], **Shashwat Shukla** [3], **Yiyin Zhou** [4], **Aurel A. Lazar** [3] and **Gonzalo de Polavieja** [5]

[1] School of Biosciences, University of Sheffield, Sheffield S10 2TN, UK

[2] Neuroscience Institute, University of Sheffield, Sheffield S10 2TN, UK

[3] Bionet Group, Department of Electrical Engineering, Columbia University, New York, NY, USA

[4] Department of Computer and Information Science, Fordham University, New York, NY, USA

[5] Champalimaud Research, Champalimaud Foundation, Lisbon, Portugal

* Correspondence: m.juusola@sheffield.ac.uk

Key Definitions:

Morphodynamic quantal sampling:

Mechanism: Neurons integrate stochastic quantal events (e.g., single photons or neurotransmitter molecules) while ultrastructural sampling units (microvilli, membranous discs, dendritic spines) undergo rapid mechanical movements and shape changes. Each sampling event is followed by a brief refractory period during which the unit cannot respond; for example, during desensitisation, a ligand-gated receptor channel remains closed even while ligand is bound.

Consequence: Mechanical–quantal coupling links motion to information sampling across time and space, increasing the precision, adaptability, and temporal structuring of neural encoding.

Active sensing:

A process in which organisms deliberately move their sensory organs or bodies to probe the environment and enhance information acquisition. These self-generated motions sensitise the sampling units of sensory receptors – for example, by diminishing refractoriness - to transform and intensify incoming signals, thereby improving encoding, perception, prediction, and behavioural control.

Highlights: Morphodynamic quantal sampling adapts with active sensing to enhance computation

- *Predictive coding and synchrony:* drives synaptic high-frequency jumping to eliminate delays, enabling predictive coding and network synchronisation.
- *Hyperacute Spatiotemporal Resolution:* sharpens rather than blurs vision, driving exceptional precision for fine-scale detection of environmental dynamics.
- *Saliency Enhancement*: makes surprising or novel inputs stand out, facilitating rapid detection.
- *Normalisation*: keeps responses consistent across a wide dynamic range by effectively performing division.
- *Noise Minimisation*: produces robust, reliable neural responses.
- *Anti-Aliasing*: suppresses aliasing artefacts and preserves signal fidelity.

Abstract

Neural computation is not performed by static circuits processing signals corrupted by noise, but by actively moving biological structures that use motion itself to sample, encode, and predict the world. Neurons are often modelled as filters that transmit information through chemical and electrical signals constrained by noise and bandwidth. However, this static view contrasts with biological reality, in which dynamical processes operate across scales, from whole-animal movements to motion at the subneural level. Here, we combine recent experimental observations with biophysically realistic modelling to show that neural information processing, beyond electrochemical signalling, is

dynamically shaped by motion across biological scales, from morphodynamic ultrastructural changes to whole-body movements. In this framework, ultrafast mechanical adjustments in cellular and synaptic structures interact with retinal, eye, head, and body motions to accelerate encoding and enhance precision. Adaptive variability in self-motion-coupled morphodynamic sampling arises from changes in response waveforms, latencies, refractoriness, and ultrastructural dynamics. This variability improves signal fidelity and extends spatiotemporal resolution, enabling neurons to generate reliable, high-speed representations with minimal delay. Thus, through active sensing, animals continuously enhance the speed and reliability of sensory representations. This perspective, in which self-generated sampling motion across multiple scales enhances encoding and perception, offers new insight into how the brain achieves efficient, predictive, and noise-resistant computation while providing a foundation for future experimental tests and biologically inspired AI designs. We first explain how motion-coupled encoding improves neural performance, focusing on edge-coding in early sensory systems. We then extend these ideas more speculatively, proposing how motion-coupled sampling may have influenced the evolution of neural architectures at multiple levels, potentially contributing to efficient predictive cognition.

Keywords: brain; information theory; stochastic sampling; synaptic transmission; cognition; predictive coding; neural synchronisation

Introduction

Shannon's information theory [1] (**Figure 1a**), which formalises how information is transmitted through a channel, provides a powerful framework for understanding and quantifying neural communication [2]. However, applying this theory to neuroscience presents significant challenges. Unlike the block diagram outlined in Shannon's original work, neurons are not static systems performing sequential, unidirectional input–output transformations with noise introduced at every step. Rather, they are *morphodynamic systems* [3] (**Figure 1b**). Their structure and function continuously adapt to enable efficient communication while being inextricably interwoven with a multidimensional representation of their life processes. Neural computation is therefore inseparable from motion - spanning ultrastructural dynamics, synaptic remodelling, and whole-animal behaviour - as constrained by genetic, physical, and algorithmic principles [4–9].
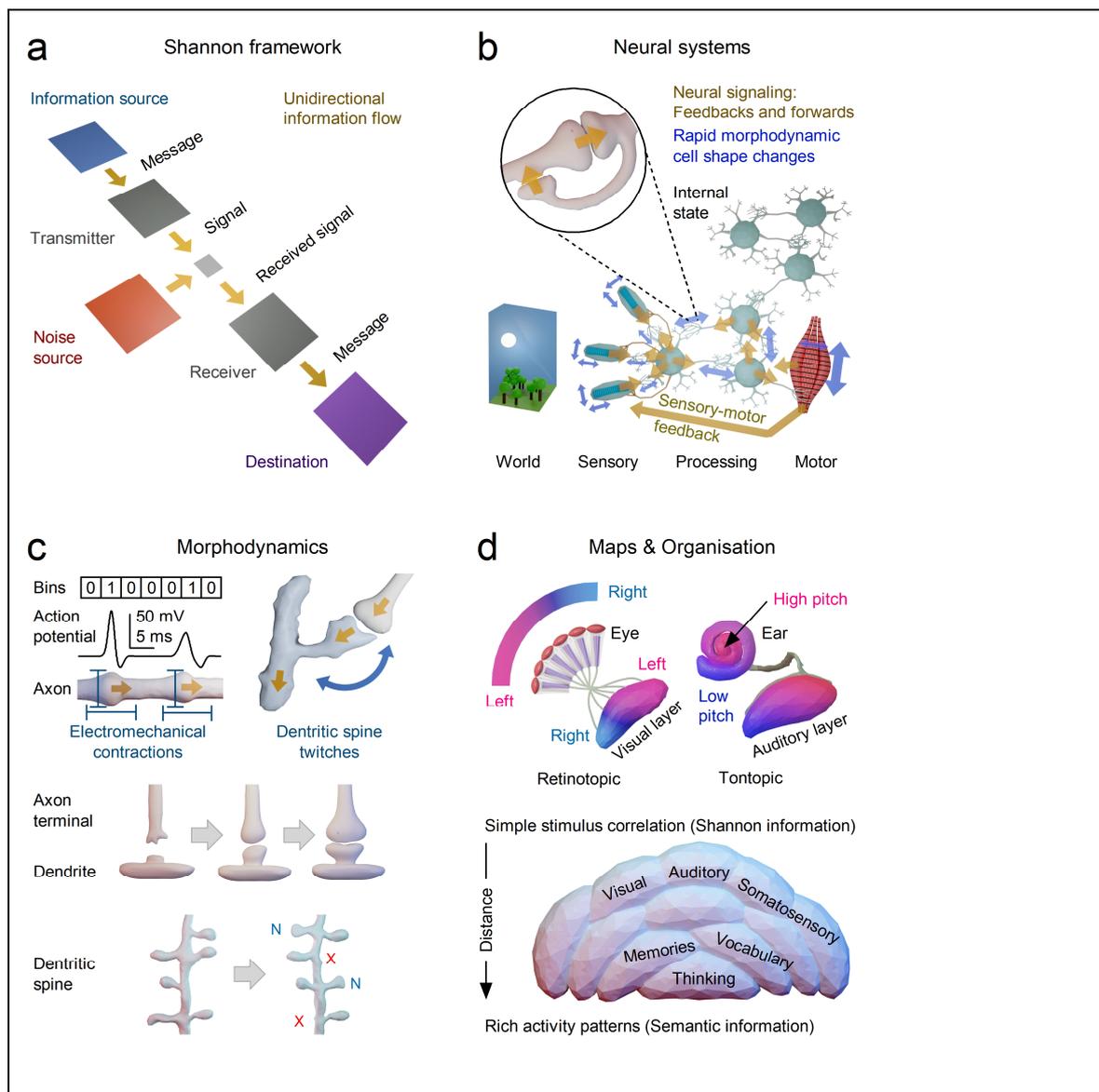
Figure 1. Changing Perspectives on Neural Information. (**a**) *Shannon framework*. Classical information theory [1] conceptualises communication as a unidirectional, stationary process in which additive noise corrupts messages transmitted from source to destination. (**b**) *Neural systems as morphodynamic networks*. In contrast, biological neural systems integrate forward and feedback signalling with continuous cell-shape dynamics [3]. Structure and function co-evolve under genetic, physical, and algorithmic constraints, and are continuously tuned by experience, enabling adaptive information processing. (**c**) *Morphodynamic signalling*. Biophysical neural communication is far richer than implied by popular dimensionality-reduction views of the neural code, which treat action potentials as digital zeros and ones within preset time bins. Neurons exhibit rapid ultrastructural changes [10–14] during electrochemical signalling—axon swelling [15] and dendritic twitches [16–19]—besides activity-dependent axon initial segment remodelling [20], synaptic growth and spine remodelling [11–13,21] (N = new spine, X = spine gone) that embed memory and dynamically regulate information flow. Information is transmitted and sampled in quantal units by compartmentalised substructures (e.g., cilia [22], microvilli [23–27], discs [28,29], boutons [13,14,30], spines [16–19]) that exhibit contractility and structure–function adaptability [3]. Though once dismissed as noise, stochastic variability enhances reliability through ensemble averaging, yielding robust, anti-aliased macroscopic signals [3,24,27,31,32]. (**d**) *Maps and organisation*. Sensory-topic maps and hierarchical organisation [33–44], illustrated here for vision (left) and hearing (right), link neural architecture to function. Developmentally encoded structure–function relationships define each neuron's position and connectivity. Deeper in the brain, responses are increasingly shaped by lateral interactions and top-down

feedback, integrating sensory input with context and memory to generate combinatorial and distributed semantic and perceptual representations of information [42,45,46].

The processes illustrated in **Figures 1b,c**: rapid photo- and electromechanical ultrastructural movements [3,15,17,23–26], synaptic growth and remodelling [11–14,19,47], biophysical forces shaping axon morphology and function [15,48], and dendritic spine modifications [17–19,47], naturally involve memory. They reflect ongoing structure–function adaptations that regulate multidirectional information flow, integrate feedback, and reduce noise [3,27,49]. At the microscopic level, neurons sample information in quantal units [3,7,27,31,32,50,51], mediated by ion-channel openings and closings within compartmentalised subcellular structures such as hair cell cilia, photoreceptor microvilli or discs, and synaptic boutons and spines. Because these sampling and transmission units adapt dynamically - moving and reshaping - and because their reaction cascades are rate-limited, the resulting quantal signals are both variable and refractory [3,7,27,31,32,50–52]. These features were once regarded as intrinsic noise [53–57] in neurons' *syntactic* information representations (**Table 1**). Recent work shows otherwise: by integrating many such variable samples, neurons generate reliable macroscopic signals that are robust, anti-aliased, and effectively noise-free [3,7,27,31,32,50,51].

Table 1. Difference between Syntactic and Semantic Neural Information.

Syntactic Information	
Definition:	Concerns the form or *structure* of signals, independent of what they *mean*.
In Neuroscience:	*Corresponds to Shannon information* - bits of data that quantify uncertainty or variability in signals.
Key Question:	How much information is transmitted?
Example:	Measuring how unpredictable a neuron's spike train is, or how many distinct voltage patterns it can encode, regardless of what those spikes represent.
Analogy:	The grammar and word count of a sentence without understanding its meaning - e.g., "The cat sat on the mat" and "The mat sat on the cat" have the same syntactic elements (words, structure) but very different semantics.
Semantic Information	
Definition:	Concerns the *meaning* or interpretation of signals within a given *context or system of understanding*.
In Neuroscience	Refers to *what the signals stand for* - their relevance to perception, expectation, or action.
Key question:	*What does the information mean* to the organism?
Example:	A spike in a neuron participating in the representation of a visual object - say, a basketball - at a precise phase of a saccade could indicate that the ball is moving along a specific trajectory toward the basket, prompting a blocking response.
Analogy:	Understanding the meaning of the sentence - not just its syntax - and using it to act appropriately.

The sensory-topic maps and hierarchical organisation of the nervous system [33–44] (**Figure 1d**) further suggest that genetic information largely predetermines a neuron's ultrastructure, connectivity, and network position during development. Yet experience continuously and dynamically refines and augments these connections, enabling the maps to self-organise as

information accumulates [45,46,58,59]. Neurons thus possess inherent structure–function knowledge about the *semantic* nature (**Table 1**) of the information they process [3]; whether specific "what" sensory inputs tied to "where" coordinates, or recalled concepts. With increasing distance from sensory surfaces, neuronal responses are shaped less by direct input and more by lateral interactions and top-down feedback from higher regions, reflecting recalled or contextually processed semantic information.

For example, recording ~30 spikes per second from a single cortical neuron during repeated test stimulation does not mean that the extrapolated Shannon information of ~10 bits per second captures its true information content. Its precise functional role within the network remains unclear. Within the genetically connected internal world map, even a single spike in that complex spatiotemporal representation can carry rich semantic meaning for ongoing perception or thought; a meaning whose full description may require tens of thousands, or under some conditions millions, of bits of Shannon information. Imagine a neurosurgeon surveying a patient's brain with a fine current probe and evoking a single spike from one neuron that triggers an immediate stream of vivid memories of long-lost childhood games [60,61].

Extrinsic factors also contribute to underestimates of neuronal capacity. Microelectrode penetrations damage cells and reduce signal fidelity [27]. True steady-state responses cannot be measured, as neural activity continually reflects adaptation, network dynamics linked to brain state (e.g., active behaviour, sleep, alertness, or ongoing thought), and physiological co-activity such as temperature regulation, respiration, hormonal secretion, and oxygenation. Thus, the act of recording itself affects the results by damaging or biasing the system's encoding state, obscuring the estimated signalling performance. Recordings are therefore never fully ergodic: much of the observed trial-to-trial variability arises from adaptive network processes rather than from pure noise. Standard analyses, which assume stationarity, misclassify these intrinsic or network-driven adaptations as additive noise. As a result, the true information transfer rates and signalling performance of central neurons exceed conservative estimates based on arbitrary spike bin sizes.

Together, these complexities challenge any attempt to reduce neural coding to simplified time series of propagating voltages treated as digital zero–one events with fixed bin sizes [62], or to estimate information rates using Shannon-idealised analyses alone [63]. They clarify why such dimensionality-reduction approaches - built on assumptions of stimulus design, stationarity, additive noise, spatiotemporal binning, or preconceived coding schemes - fail to capture the true flow and utilisation of neural information. Likewise, simplified neural filter models based on tuning curves, impulse responses, or static connectomic pathways cannot reproduce the in vivo richness of morphodynamic communication. Even widely used Gaussian stimuli [7,24,27,64], intended to estimate an upper bound on information transfer, prove misleading when analysing and modelling neural performance, as they exacerbate refractoriness and restrict signalling [7,24,27].

To advance understanding, form and function must be considered together: a neuron is a multilayered, morphodynamic, algorithmic representation of its intertwined workings and operations. We argue that moving beyond classic engineering approaches to biophysically accurate, multiscale morphodynamic neuron models is essential. Morphodynamic stochastic quantal refractory sampling models, though demanding detailed experimental knowledge and time-consuming to construct, inherently capture mechanisms of adaptation and yield realistic predictions across stimulus conditions.

This review is organised as follows. The first part surveys sensory encoding and adaptation, focusing on "edge computing" in the peripheral visual system and on how efficient information capture and processing have evolved to use motion: *morphodynamic quantal sampling* with *active sensing* to maximise sensory information. The second part broadens the discussion to examine how these efficient coding strategies extend to perception, cognition, and intelligence - through parallel, combinatorial, and distributed high-dimensional semantic information representations [3,65] - the likely mechanistic framework for memory and mind.

1. Part I: Local Sampling and Processing – Fast, Reliable Encoding of the Variable World

Presumably, as sensory ecologies grew more complex and environments more dynamic, it became evolutionarily advantageous for animals to perform critical information sampling and processing directly at the sensory surface rather than deep within the central brain. Just as modern distributed computing gains efficiency from edge processing, biological systems achieve speed, robustness, and energetic efficiency by maximising information extracted from time-dependent signals at their sensory edges [3,8,24,27,66,67] (**Figure 2**). Each sensory matrix is represented in the brain's own sensory topic maps [33–36,68,69] in four dimensions (x, y, z, and time), providing an internal reference frame for multiscale, synchronous (and, as discussed later, predictive [27]) encoding of space directly in time [24–26,70–74] across the entire sensory system.

Our eyes, for example, connect to the brain only via long optic nerves (**Figure 2a**), yet the retina itself already performs morphodynamic computation [24,26–29]; transforming photons into structured spatiotemporal codes through multiscale quantal sampling and processing to maximise sensory information [24,27]. This involves saccadic eye movements [24,27,74–76], photomechanical micro-motions [23–26,28,29] that accentuate perception, and synaptic adaptive quantal information allocation across local circuitry [5,10,27,49,77–80]. Insects extend this principle further (**Figure 2b**): in stalk-eyed flies, optic lobes at the ends of elongated stalks sit adjacent to the antennae [81], enabling local coordination of visual, auditory, olfactory, wind, tactile, and gravitational cues before transmission to the central brain.

Such distributed morphodynamic computation minimises transmission delays, energy costs, and the risk of information degradation or overload (**Figure 2c**). By combining ultrafast, phasic (saccadic, motion-based) electrical, mechanical, and analogue signalling at the sensory interface [3], evolution has effectively implemented "neurobiological edge computing." This transforms vast, noisy environmental fluctuations - for example, astronomically varying day–night light intensities following Poisson statistics [7,24,82,83] - into time-locked, predictive information streams for immediate perception and attentional control [27,84]. These pre-processed signals then support higher-order integration and analysis in cognitive processes such as thinking, planning, dreaming, and recall.

Encoding sensory information poses multiple challenges. For photoreceptors, the most demanding is likely the vast logarithmic diurnal luminance range [31] (**Figure 2d**). Even under midday sunlight, fluctuating illumination - caused by motion, shadows, or occlusions - can alter retinal images by 10^4–10^6-fold. Before photons reach the receptors, pupil mechanisms and screening pigments dynamically adjust this range by at least another 10^2-fold [7,85,86]. Yet photoreceptors must encode information in local photon-flux changes, which can reach tens of millions of photons per second, and they do so by representing contrast - relative reflectance differences between objects, rather than absolute brightness - employing adaptive gain control [87–90].
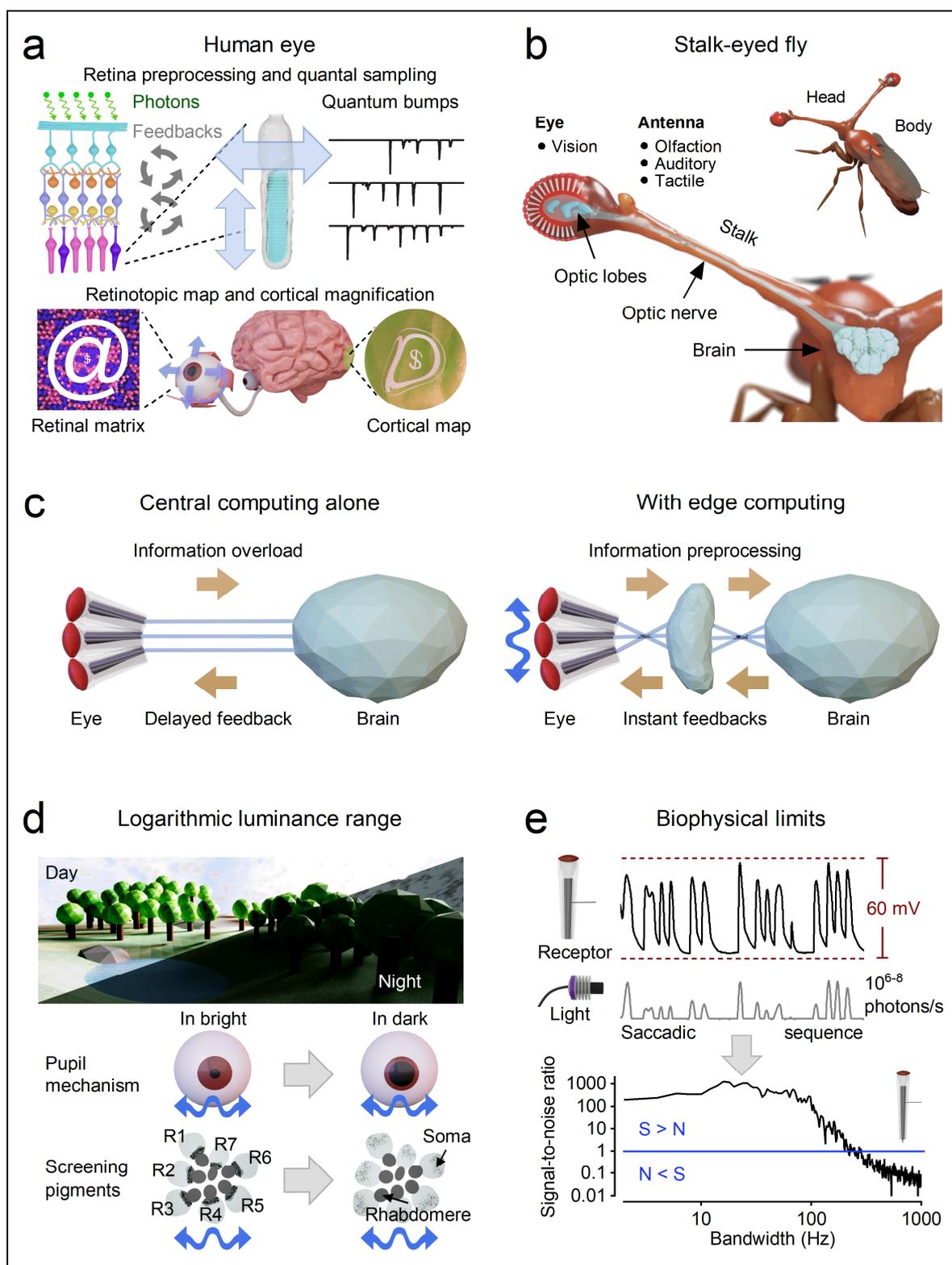
Figure 2. Benefits of Neurobiological Edge Computing. (**a**) *Human eye*. Retinal circuits preprocess light by photomechanically sampling [29] quantal photons and neurotransmitter molecules, and by providing local feedback, transforming photons into structured spatiotemporal codes before signals are transmitted via the optic nerve to retinotopic maps [33,69,91–93], where meaningful correlations are magnified in cortical representations. (**b**) *Stalk-eyed fly*. Insects extend edge computation further: stalk-eyed flies position their optic lobes at the ends of elongated stalks [81], close to other sensory organs (antennae), allowing multisensory integration and local preprocessing before transfer to the central brain. (**c**) *Central vs. edge computing*. Without local processing, central circuits alone face information overload and delayed feedback. By contrast, saccadic (blue wiggly arrow) motion-based edge computing distributes morphodynamic processing across the system, providing rapid feedback

while minimising delay, energy expenditure, and loss of information fidelity [27]. In nervous systems, local connections within each processing layer are genetically preconfigured to enable efficient information integration and feature extraction [3]. Edge computing, therefore, redistributes processing of salient environmental changes across neural channels, maximising the flow of sensory information and enabling rapid, distributed computation across the network. (**d**) *Logarithmic luminance range*. Photoreceptors operate across enormous day–night intensity differences (~10^4–10^8-fold). Pupil mechanisms in vertebrate eyes and screening pigments in the fly R1-R7/8 photoreceptors [7,85,86] (seen from above through the ommatidium lens) expand the effective dynamic range, while receptors primarily encode contrast, not absolute luminance, through adaptive gain control, including saccadic eye/head/body movements (blue wiggly arrows). (**e**) *Biophysical limits*. Sensory neurons are constrained by the electrical properties of their membranes, limiting the fly photoreceptor voltage responses to ~60 mV amplitude and ~1,000 Hz frequency [24,27,94,95]. Efficient coding within these bounds utilises saccadic movements that maximise information, transforming noisy environmental fluctuations into reliable, predictive input streams [24,27].

To represent visual objects reliably across astronomical intensity variations, photoreceptors, like other sensory neurons, are constrained by intrinsic biophysical limits. Their resistive and capacitive membrane properties restrict voltage signals to ~60 mV and ~1,000 Hz (**Figure 2e**) [3,27]. How sensory neurons achieve efficient coding within these bounds remains a long-standing open question.

1.1. Historic Recap: Neural Models with Additive Noise and Stationarity Assumptions

Owing to technical limitations, early electrophysiological studies typically examined photoreceptors' (or other sensory neurons') absolute sensitivity, seen in quantum bumps evoked by single photons under dark adaptation [52,96] or macroscopic responses to step-like light increments and decrements delivered for fixed durations under controlled conditions [97–100]. In these experiments (**Figure 3a**), the eye was broadly conceptualised as a camera: photoreceptors formed the pixelated grain of the film, adapting to capture sequences of still images and redistribute that information within the retinal network for efficient repackaging as parallel spike trains to the brain. Neural activity was often recorded from reduced preparations, such as flattened, dissociated retinae maintained at room temperature.

In reality, neurons sample and transmit information more rapidly and efficiently at physiological temperatures [101,102] (mammalian body temperature: 36-38 °C), and visual scenes are dynamic, requiring continuous adaptation and control by eye movements to shifting patterns [24,26,27,74,75]. Nevertheless, even under such unnatural recording conditions, early findings implied that during steady-state adaptation, visual neurons redistribute their response amplitudes to code contrast over a logarithmic range of intensities [87]. Adaptation was defined as a shift in the characteristic response function ("sigmoidal curve") across light levels while broadly preserving its shape, but this interpretation oversimplified the temporal dynamics of responses, and any information in their actual waveforms.
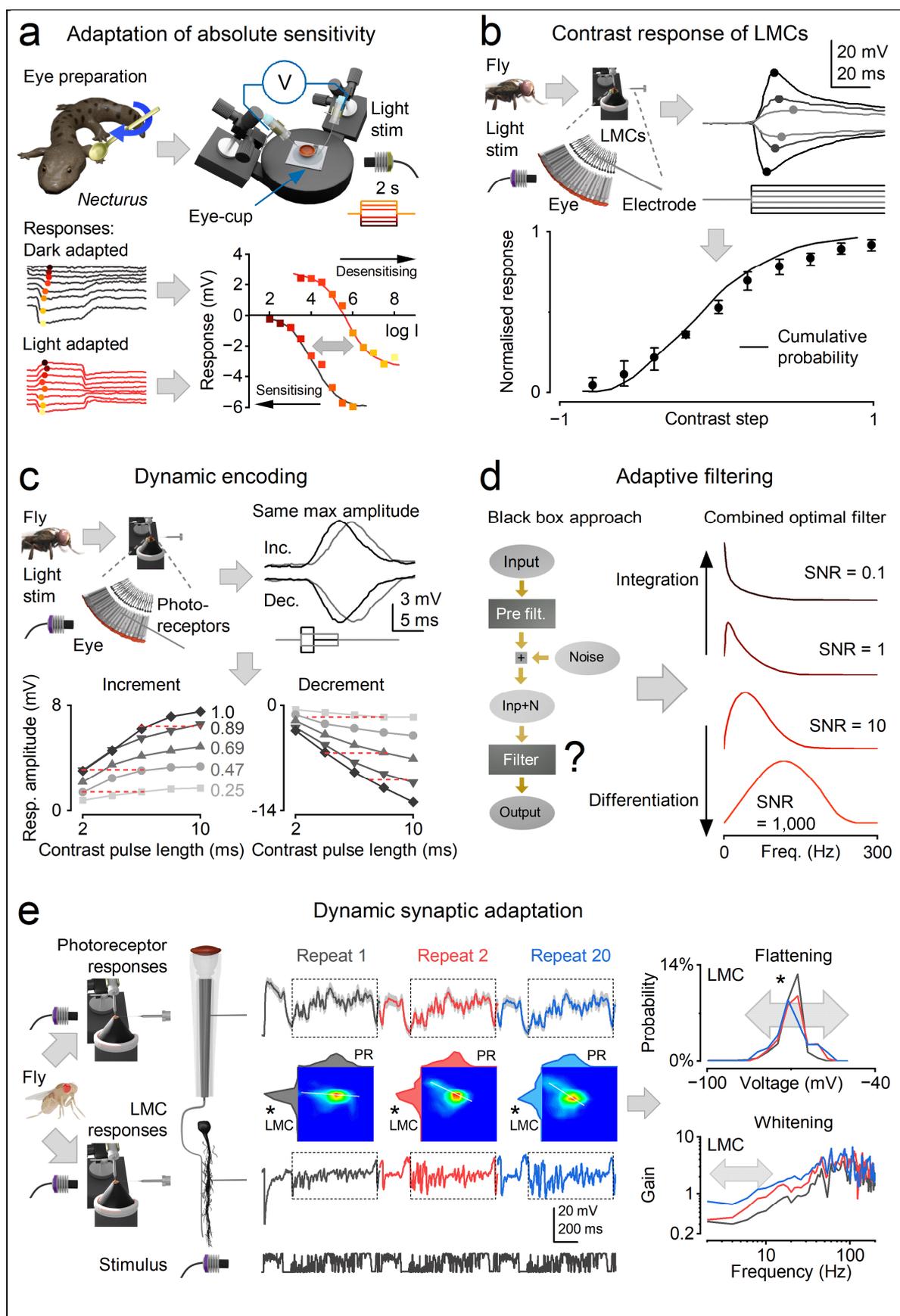
Figure 3. Historic Shift in Assumptions and Ideas for Efficient Encoding. (**a**) *Adaptation of absolute sensitivity*. Early electrophysiological studies characterised photoreceptor responses to static light increments or decrements using steady-state adaptation curves [97]. These sigmoidal functions shift with light intensity, suggesting logarithmic contrast coding but oversimplifying real temporal dynamics. (**b**) *Contrast-response normalisation in*

large monopolar cells (LMCs). It was proposed that fly visual neurons adapt by scaling their contrast-response amplitudes according to a cumulative natural contrast distribution [103]. (**c**) *Dynamic contrast encoding by response phase*. Recordings show that neurons can generate the same amplitude responses to either short bright pulses or long dim pulses, challenging the static contrast normalisation hypothesis in (**b**) and implying dynamic, phase-based rather than static amplitude-based encoding [88]. Moreover, cumulative contrast distribution is not universal but varies across scenes [104], further undermining the case for static contrast normalisation. (**d**) *Adaptive filtering using the black-box formalism*. Signal analyses revealed that neural gain shifts from low-pass filtering in dim light to high-pass filtering in bright light, making information transmission more efficient across varying illumination levels [66,67,105]. (**e**) *Dynamic synaptic throughput optimisation.* LMC responses to repeated naturalistic light-intensity patterns adapt continuously (shown for the 1st, 2nd and 20th responses) to use their amplitude and frequency ranges more evenly, through whitening and flattening [80]. These dynamic information-maximisation processes, also reported downstream in spiking responses [106], reflect a dynamic balancing of feedforward and feedback synaptic loads (LMC feedback to photoreceptor axons [5,49,78]), quantified by the joint probability between photoreceptor and LMC voltage responses (the heat-plots in the middle). The white line indicates the continuously changing synaptic average gain.

From an information-theoretic perspective, neural adaptation is most efficient when each possible signal is used equally often [80,103,106], thereby maximising what the eye can transmit and the brain can interpret. In principle, the eye should adapt to regular or predictable patterns in natural scenes [8,107], such as static contrast (relative intensity differences between brighter and darker image features) and colour features that remain consistent across scales (e.g., shapes that appear similar whether large or small, near or far). By rapidly adapting to or learning the frequency of these patterns, the brain can concentrate on the most significant ones, discard redundant or repetitive information, and direct attention to surprising or behaviourally relevant stimuli. In essence, the retinal circuitry was expected to perform redundancy reduction [8] in the form of a simple contrast normalisation process [103] - a spatiotemporal reallocation of information that enhances object boundaries and saliency of underutilised features - comparable to how digital image processing sharpens a raw camera image.

These principles initially suggested that neurons adapt by scaling their strongest responses, such as maximum amplitudes or firing rates, in relation to contrast pulses, a phenomenon observed in blowfly large monopolar cells [103] (LMCs; **Figure 3b**) and in vertebrate retinal ganglion cells [87], under specific experimental conditions. Subsequent studies, however, revealed that insect visual neurons can produce the same maximum response amplitude with a brighter but shorter contrast pulse [88] (**Figure 3c**), and respond even more strongly to sequences of naturalistic contrast changes [7,49,80,104]. This pointed to a more dynamic, phase-based form of encoding, rather than strictly static amplitude normalisation (i.e., distinguishing slow from fast changes). Such findings highlight the difficulty of generalising results obtained under narrowly defined stimuli and stationarity assumptions to the real-world dynamics of continuously changing scenes.

To better quantify information flow in steady-state adapted systems, researchers turned to Shannon's original theory [1] and signal-analysis methods from engineering, correlating contrast stimuli with neuronal voltage responses [66,67,77,95,108]. The goal was to characterise sensory encoding in individual neurons *using a black-box input–output formalism*, reducing the system's dimensionality to generalise its dynamics across specific stimulus sets. These analyses showed that adaptive gain control does not employ a simple redundancy-reduction procedure [8], but instead integrates incoming information in dim conditions (redundancy-enhancement) and differentiates it in bright conditions (redundancy-reduction) [66,67,77,95,108]. Thus, neural representations of visual objects are expected to exhibit low-pass characteristics in dim conditions and high-pass characteristics in bright conditions [66,67,77,108] (**Figure 3d**). Such dynamic filtering would enable neurons to use their limited bandwidth more efficiently across a wide range of luminance levels, thereby maximising sensory information.

In the peripheral fly visual system, the principles of sensory information maximisation were first tested using contrast flashes (impulses) or Gaussian white noise (GWN) contrast stimuli superimposed on a steady light background [67,77,95,108–111]. GWN was chosen because, in stationary systems (as in classic engineering applications), it provides a statistically well-defined, uncorrelated input that uniformly samples all temporal frequencies, allowing for the precise estimation of a neuron's linear and nonlinear response properties - its receptive field or transfer function under controlled conditions. The stimulus intensity, spanning approximately five log units (from tens to millions of photons per second), was adjusted with neutral-density filters to mimic illumination from dim (low signal-to-noise ratio) to bright (high signal-to-noise ratio) conditions [101,112]. Researchers then quantified adaptive filtering by analysing impulse responses and frequency response functions at each luminance level, applying both linear and nonlinear signal analysis methods [77,105,108,111,113]. Finally, to estimate the efficiency of information maximisation, repetitive stimulation was applied to measure each neuron's signal-to-noise ratio, which was then converted into information transfer rate estimates [10,101,105,111,112] applying Shannon's formula [1]. However, it soon became evident that these stimuli were rather unnatural and inefficient [64,101,108,112–115]; they did not utilise the tested neurons' limited amplitude and frequency ranges to their full extent [7,24,31,64,115]. Clearly, the studied neural systems were anything but stationary.

Later investigations began to incorporate natural image statistics and new stimulation modes [49,79,80,116–122], revealing continuous dynamic synaptic adaptations that improve encoding efficiency and information flow (**Figure 3e**). However, the methodologies - still grounded in black-box formalism, additive noise and "relative" stationarity assumptions with filter-based analyses - remained essentially unchanged (**Figure 3d**). Only a few researchers began to consider the role of active sampling by motion [110,117,118,123] and dynamic speed adaptation in sensory information acquisition and processing [115].

Whilst these studies advanced generic methods to quantify adaptation and neural encoding under specific conditions, using approaches that proved successful in engineering, they offered little mechanistic insight into *how neural adaptation actually occurs*, beyond pointing to dynamic or static nonlinearities without explaining their physiological basis. They gave even less understanding of the underlying biophysics by which neurons, through multiscale evolutionary structure–function adaptations, sample and process sensory information as spatiotemporal sequences of quantal events, such as photons, scent molecules, or neurotransmitter molecules.

1.2. Information Capture Through Morphodynamic Parallel Sampling

Sensory neurons typically have only one chance to detect and encode an environmental change, since such changes rarely recur identically. Through evolutionary adaptations of their structure, function, and active sampling behaviours, they perform this task with remarkable efficiency and accuracy, generating neural responses that maximise information capture [27,31]. In photoreceptors and first-order visual interneurons, this encoding relies on parallel morphodynamic refractory quantal sampling, tuned by visual motion: photomechanical photoreceptor microsaccades [23–27], retinal muscle movements [24,124,125] and the bursty dynamics of active sensing [27,31,126], to exploit the statistical structure of the environment, consistent with the first principles of edge computing.

Biophysically realistic, multiscale morphodynamic models replicate this encoding and its coupling to active behaviour (self-generated retinal, eye, head, and body movements [24–27,124,126]) with high fidelity, capturing both neuronal form and function. Unlike the classic black-box filter models, they directly explain the synergetic mechanisms of neural adaptation, from molecules to the whole encoding network, and yield accurate estimates of information flow and energy consumption for any light pattern. Consequently, models such as those for the housefly's (*Musca domestica*) morphodynamic neural superposition system [27] (**Figures 4a, b**) inherently capture ("*for free*") the mechanistic components and key features of the code:

A. Neural adaptation - Macroscopic voltage responses can be predicted without free parameters by knowing the number of sampling units (e.g., ~54,000 light-sensitive microvilli in an average housefly photoreceptor), their morphodynamic properties, and the waveform, latency, and refractoriness distributions of the quantum bumps they produce [3,7,24,26,27,31,32,101,109,112,127,128].

- **Photomechanical transduction** - Reactions inside microvilli induce photoreceptor microsaccades [23,24,26,129] that enhance visual acuity by encoding space in time through rapid, auto-regulated (adaptive) photomechanical motion [23–29,129]. The brighter the light change, the larger the movement [23,24,26,27]. These microsaccades shift and narrow the photoreceptor's receptive field [24,26,27], thereby driving predictive coding (**Figures 4c**, **e**), especially during saccadic behaviours [26,27].

- **Hyperacute spatiotemporal resolution** - Photoreceptor microsaccades enable detection of fine-scale environmental changes with exceptional precision, far finer than the ommatidial pixelation of the compound eye [3,24,26,27] (**Figure 4d**).

- **Contrast constancy (signal normalisation and response invariance)** - Refractory quantal sampling implements divisive normalisation [31,32], maintaining consistent waveforms across wide (logarithmic) intensity ranges [49,80,115,130], so that photoreceptors evoke similarly shaped responses to contrast changes under different illumination conditions.

- **Noise minimisation** – Integration of variable quantum bumps into macroscopic responses yields robust and reliable estimates of the variable world [3,7,24,27,31,32].

- **Resistance to saturation** - Because of stochastic refractoriness, it is difficult to knock out all microvilli at once, since some are constantly returning to the available pool [7,24,27,31,32].

- **Anti-aliased signals** - Stochastic quantal sampling suppresses aliasing artefacts [3,31,32], reducing oscillations so that macroscopic voltage responses remain stable to sudden stimulus changes.

- **Maximum efficiency** - Macroscopic voltage responses to fast saccadic inputs maximise amplitude and whiten frequency ranges [3,24,27].

- **Self-similarity** - Time-normalised waveforms of macroscopic voltage responses preserve temporal patterns across scales [3,80,115].

- **Saliency enhancement** - Because of refractory sampling units, novel or surprising inputs are naturally emphasised [3,7,31,32]. Events that cause the largest changes in microvillar activation (bump-rate increments or decrements), such as those triggered by saccadic eye movements, produce macroscopic voltage responses with the greatest amplitude and frequency utilisation, and thus the highest information content [3,7,31,115].

B. Phasic predictive signal transmission - During saccadic vision, synaptic high-frequency jumping shifts transmission toward higher frequencies, generating strongly phasic, near delay-free LMC responses [27] (**Figure 4e**). Note in this concept, predictive coding, which emerges intrinsically from motion-coupled sensory encoding, refers to the biophysical phase alignment generated by morphodynamic sampling and synaptic high-frequency dynamics, not to hierarchical error-minimisation frameworks [131–133] or efference-copy cancellation mechanisms [134–136].

C. Reliable information rate estimates - Enables accurate quantification of information transfer [3,24,27,115].

D. Accurate energy consumption estimates - Enables dynamic, internally consistent estimation of metabolic energy usage and neural information for encoding arbitrary stimulus patterns, within the same biophysically grounded modelling framework [3,7].
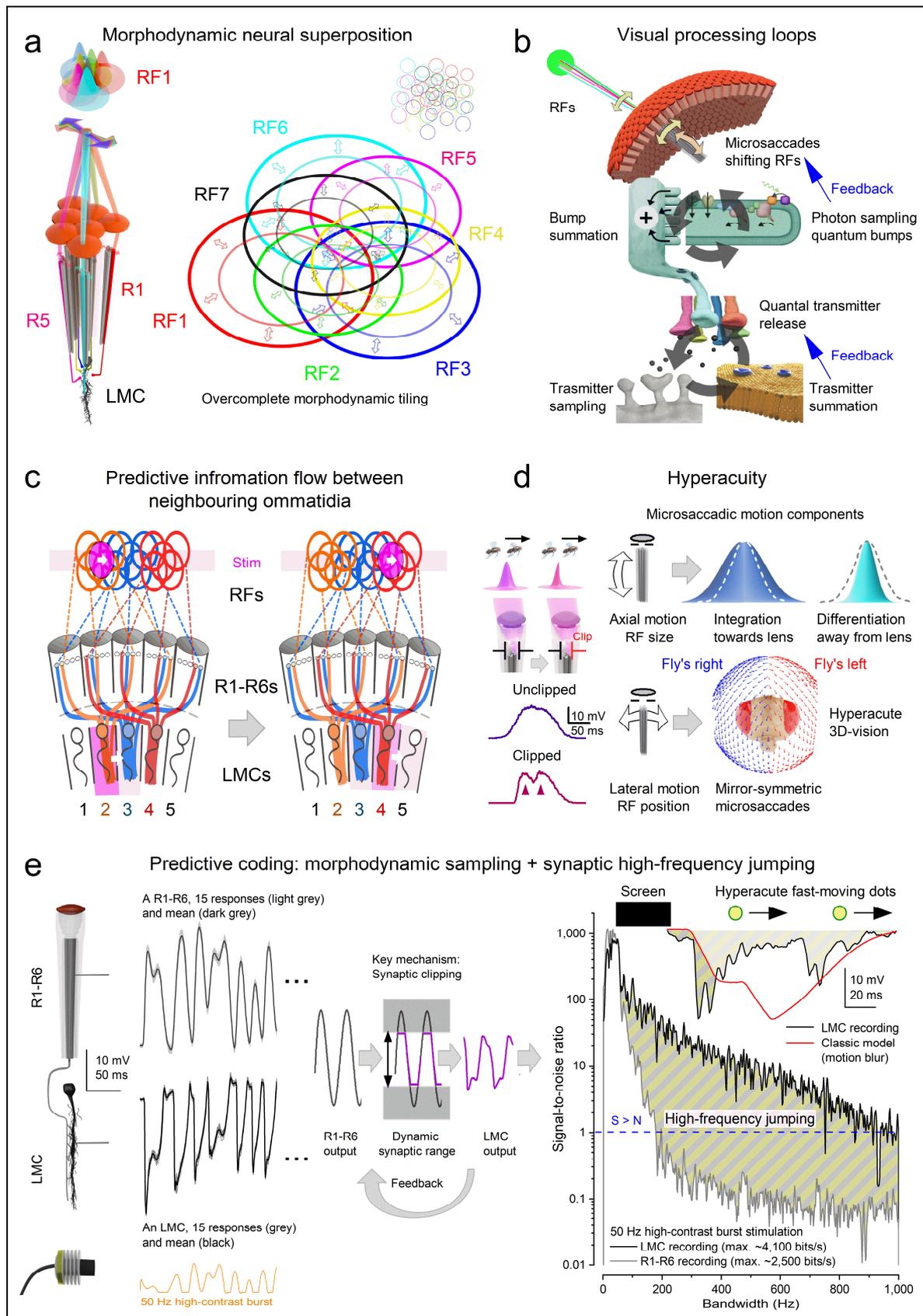
Figure 4. A biophysically realistic multiscale morphodynamic neural superposition model of a fly's peripheral vision explains adaptation and hyperacute predictive coding. A mechanistic framework linking photomechanical sampling, synaptic dynamics, and predictive encoding in the peripheral visual system. (**a**) **Overcomplete morphodynamic sampling architecture.** R1-R7/8 photoreceptors from neighbouring ommatidia contribute to a shared large monopolar cell (LMC), forming a flower-like mosaic of partially overlapping

receptive fields (RFs). Each LMC therefore reflects a composite, overcomplete sampling matrix rather than a single static point in space. Because individual photoreceptor RFs differ slightly in orientation and position, and undergo dynamic shifts during phototransduction, the effective LMC receptive field can transiently narrow and displace in response to spatiotemporal light patterns (see microsaccade components in **d**) [26,27]. (**b**) **Coupled photomechanical and synaptic feedback loops**. At the photoreceptor level (top), light-triggered microvillar activity produces ultrafast axial and lateral microsaccades that dynamically adjust receptive-field position and extent while shaping stochastic quantum bump sequences. At the synapse (bottom), voltage-dependent histamine release from R1-R6 photoreceptors [137–141] drives hyperpolarising responses in LMCs, which in turn provide excitatory feedback to photoreceptors [49,142]. This reciprocal interaction balances synaptic gain, supports phasic transmission, and stabilises information flow during rapid contrast changes. (**c**) **Lateral predictive information flow between neighbouring ommatidia**. Because LMC receptive fields overlap in an overcomplete arrangement, activation of one unit by a moving object simultaneously initiates stimulation in neighbouring channels [27]. Information therefore propagates laterally in a spatiotemporally structured manner aligned with object motion. In addition, mechanical coupling among photoreceptors within an ommatidium allows a microsaccade in one receptor to alter light access to adjacent rhabdomeres, recruiting additional channels that would otherwise remain inactive. Together, these structural and mechanical interactions enable anticipatory signal spread across the network. (**d**) **Morphodynamic mechanisms supporting hyperacuity**. Lateral components of photoreceptor microsaccades can transiently clip the entering light beam at the aperture formed by cone and pigment cells, effectively narrowing the receptive field during motion. Axial displacements of the rhabdomere, away from the lens, further narrow angular light collection. These motion-dependent changes increase spatial discriminability, enabling separation of closely spaced moving objects beyond the anatomical interommatidial limit [24,26,27]. Mirror-symmetric microsaccades in the two eyes enhance frontal binocular precision, contributing to hyperacute stereoscopic vision. (**e**) **Synaptic high-frequency jumping and delay minimisation**. During rapid contrast bursts or saccadic stimulation, photoreceptor signals can transiently exceed the adaptive synaptic operating range [27]. Partial clipping within this dynamic range redistributes spectral power toward higher frequencies, a process termed *synaptic high-frequency jumping* [27]. As a consequence, LMC responses become strongly phasic, extend toward near-kilohertz bandwidths, and peak with minimal effective delay relative to photoreceptor input, supporting predictive transient signalling that reduces motion blur (inset). Morphodynamic model simulations reproduce the high resolvability observed in intracellular recordings of moving stimuli, whereas static filter-based formulations (classic models) do not account for these phase-advanced responses (red trace) and their predictions are severely contaminated by motion blur. Additional interacting mechanisms are discussed at the end of Part I. Here, *predictive coding* refers specifically to the biophysical phase alignment generated by morphodynamic sampling and synaptic high-frequency dynamics. It does not invoke hierarchical error-minimisation frameworks [131–133] or efference-copy cancellation mechanisms [134–136], but instead emerges intrinsically from motion-coupled sensory encoding. Figure adapted from [27].

Next, we compare simulations with experiments to show step by step how adaptive encoding emerges during active sensing in natural viewing, driven by saccadic eye-, head-, and body-movements. We trace the pathway from photon sampling in photoreceptors, through synaptic transmission, to signal integration in large monopolar cells (LMCs; the first interneurons of the fly visual system) and assess the resulting benefits for vision.

1.3. Structure and Function in Photoreceptors

In flies, as in most animals, photoreceptor cells are highly polarised, with distinct light-sensitive and light-insensitive regions [129,143,144] (**Figure 5a**). Their R1–R8 photoreceptors resemble toothbrushes positioned inside an ommatidial cup, with a curved lens on top that seals the cup and focuses incoming light onto their light-sensitive parts, the rhabdomeres. Each of these "brush ends" contains tens of thousands of bristles: the microvilli. Each microvillus is an ultra-compartmentalised photon sampling unit densely packed with rhodopsin and the complete phototransduction machinery [27,32]. Photon absorption activates a G-protein cascade that opens TRP/TRPL-ion

channels [129], causing a depolarising elementary response, a quantum bump. Conversely, the light-insensitive region houses the cell body, axon, and synaptic machinery transmitting signals to the next optic neuropiles, the lamina [27,49,80,145] (R1–R6) or medulla (R7/R8).

1.3.1. Microvilli Are Photomechanical (Rapidly Moving) Sampling Units

Each microvillus, approximately 30,000 in the average fruit fly (*Drosophila melanogaster*) [32] and about 54,000 in the average housefly (*Musca domestica*) [27] R1-R6 photoreceptors, acts as a photon counter. Absorption of a single photon activates the phototransduction cascade in which an early step cleaves PIP_2 in the microvillar membrane [23,129] (**Figure 5a**, right). When this occurs across thousands of microvilli simultaneously, the combined effect contracts the photoreceptor, generating an ultrafast microsaccade [23,24,27,129]: a 0.2–1.2 μm movement of the photoreceptor, with both axial and lateral components. Inside each light-activated microvillus, the cascade then opens ~15 TRP/TRPL channels [32,129], driving cation influx and producing an elementary response, a quantum bump [32,101,112,129]. Because photoreceptor microsaccades arise directly from early phototransduction reactions, they are an intrinsic feature of compound eye vision. Without this process, microvillar photoreceptors could not generate quantum bumps, rendering insects blind [3,129].

Although the precise gating of TRP/TRPL channels remains debated [129] (**Figure 5a**, right), the mechanisms are sufficiently well understood to support molecularly explicit, stochastic multiscale quantal sampling models that closely match intracellular recordings (**Figure 5b-f**). These confirm that vision exploits stochasticity: variable quantum bumps integrate to form reliable, anti-aliased macroscopic responses across dynamic light conditions [7,24,27,31,32].

1.3.2. Morphodynamic Rules for Photoreceptor Light Sampling

A fly photoreceptor is a fallible photon counter - its efficiency in converting photon absorptions into quantum bumps depends on light history (**Figures 5b**) - yet it generates predictable macroscopic responses (**Figure 5c**), in which encoding tracks the signal-to-noise ratio and spatiotemporal patterning of the light stimulus [31]. A few core rules can capture its generic adaptive behaviour:

- A single microvillus (sampling unit) can produce only one quantum bump (sample) at a time [32,86,127,146–148].
- After producing a quantum bump, a microvillus remains refractory (unavailable) for up to hundreds of milliseconds (**Figure 5d**, inset); during this period, it cannot respond to further photons [32,147,149–151].
- Quantum bumps from tens of thousands of microvilli (**Figure 5b**) sum to produce the macroscopic response [31,32] (**Figure 5c**).
- Quantum bumps adapt (**Figure 5e**). They become smaller as light intensity increases [32,101,109,112,129] (inset).
- Microvilli availability (quantum efficiency) sets a photoreceptor's maximum sample rate (quantum bump production rate), adapting the macroscopic response to the stimulus [31,32,86] (**Figure 5d**).
- The instantaneous change in quantum bump rate (**Figure 5b**, right) directly sets the amplitude of the ongoing photoreceptor microsaccade [24,27,129], with bump-rate increments contracting and decrements elongating the photoreceptor [24,26,27] (**Figure 4d**).
- The photoreceptor's lateral and axial (contraction-elongation) microsaccade movement components shift and narrow its receptive field in visual space, rapidly autoregulating light input [24,26,27] (**Figure 4a**).

Figure 5. Stochastic refractory quantal sampling of naturalistic contrast changes by a *Drosophila* R1–R6 photoreceptor. (a) The retinal sampling matrix of *Drosophila* compound eyes. Each eye contains about 780 ommatidia. Within each ommatidium, every R1–R6 photoreceptor samples photon influx through ~30,000 microvilli that form its photosensitive rhabdomere. Each microvillus is compartmentalised to support a complete phototransduction cascade [23,24,129]. These reactions - from photon absorption to the opening of ion channels that generate an elementary response, a quantum bump (upper half of the schematic microvillus) - can be accurately modelled using stochastic differential equations [24,32,127,128,148] (block diagram shown in the

lower half). TRP/TRPL channel activation, leading to a quantum bump, is likely regulated by the physical effects of PIP2 depletion: PLC-mediated removal of the bulky, charged PIP2 headgroup reduces local membrane area and crowding, producing a photomechanical contraction of microvilli [23,129]. When this occurs across many microvilli simultaneously, it generates an ultrafast photoreceptor microsaccade with prominent axial and lateral components [24–26] (**Figure 4d**, grey double arrows). (**b**) Photon influx representing light-intensity changes in the environment triggers quantum bumps of variable sizes and timing in individual microvilli (three highlighted) after absorption by rhodopsin molecules. These bumps summate to produce the macroscopic voltage response shown in (**c**). (**c**) Normalised average voltage responses (n = 100) of real and simulated photoreceptors to the same naturalistic contrast time series sequence show nearly identical waveforms under both dim and bright illumination [31,32], demonstrating relative contrast constancy [31,32,115,130]. (**d–f**) During brightening: (**d**) Quantum efficiency (photon-to-bump conversion) decreases as more microvilli enter a refractory state for 40–500 ms after photon absorption. (**e**) Despite this reduction, the overall bump rate (solid line) increases until it is stabilised by the falling quantum efficiency, while the mean bump amplitude (dashed line) decreases. (**f**) Information transfer rate scales with bump rate, allowing voltage responses to represent naturalistic contrast changes accurately across illumination levels. Although absolute contrast gain increases with light intensity, the temporal structure of the transmitted signal remains nearly invariant, as shown by the normalised responses and the simulations to the naturalistic light-intensity time series in (**c**). Figure adapted from [31].

In dim conditions of low photon counts, refractoriness plays little role, and every absorbed photon evokes a quantum bump [7,24,31,32,127,148]. The probability that the same microvillus within a rhabdomere, out of a pool of tens of thousands, would absorb another photon during its refractory period (~40–500 ms) is vanishingly small. Thus, quantum efficiency in dim environments approaches 100% (**Figure 5d**). Conversely, in bright light, because most microvilli have recently absorbed a photon, quantum efficiency can drop to as low as 0.01% [7,24,31,32,127]. Consequently, in *Drosophila* R1–R6 photoreceptors, each containing about 30,000 microvilli, refractoriness limits the maximum bump-production rate across the broad daylight range (~10^6–10^9 photons/s mm^{-2}) from ~1 × 10^5 (for the naturalistic test stimulus [7,31,32] shown in **Figure 5e**) up to ~1 × 10^6 quantum bumps/s [7,24,31,32] during saccadic contrast bursts [24]. This sampling constraint effectively performs a divisive normalisation, and together with the dynamic reduction in quantum-bump amplitude under brightening light [101,109,112], provides *neural contrast constancy* [31,130] *already at the sensory surface*, by generating similar-looking responses to naturalistic light changes across a wide intensity range (**Figure 5c**). Together, refractoriness and quantum-bump adaptation, as coupled with microsaccades (photomechanical movements), enable photoreceptors to encode visual information rapidly and efficiently over a wide dynamic range (**Figure 5f**). Thus, morphodynamic edge computing ensures neural code consistency from eye to brain.

1.3.3. What Governs the Information Transfer Rate of Macroscopic Responses?

The fundamental logic of quantal sampling of temporal light stimuli (light intensity time-series patterns) can be captured without invoking molecular or morphodynamic detail [31] (**Figure 6**). A photoreceptor's macroscopic voltage responses - closely reproducing measured waveforms and information transfer rates across light stimuli - can be simulated with a minimal stochastic photon-sampling model defined by four parameters [7,24,26,27,32]:

- Number of microvilli per rhabdomere (~30,000 in case of *Drosophil*a R1-R6 photoreceptors)
- Quantum-bump waveform (average shape and duration at ambient intensity)
- Latency distribution (timing jitter before each bump)
- Refractoriness distribution (duration of microvillar unresponsiveness after a bump)

In this framework, each absorbed photon triggers a quantum bump. Its waveform and latency are drawn from the respective distributions in one microvillus, after which the microvillus enters a brief refractory period [7,24,26,27,32].

Active sensing motion in natural environments generates bursty visual input (saccades followed by fixations; **Figure 6a–d**) with intermittent darker intervals [24]. These brief troughs allow microvilli to recover between contrast bursts, enabling rapid and large changes in quantum bump rates and thereby maximising information transfer [24,27]. By contrast, Gaussian white-noise (GWN) stimuli (**Figure 6e–h**) keep photoreceptors near a constant mean brightness, leaving many microvilli refractory [7,24,27]. This reduces bump-rate modulation and information throughput: fewer microvilli contribute, leading to smaller responses that carry less information. Thus, the quantum efficiency of the photoreceptor's microvillar sampling matrix (the rhabdomere) is continuously and morphodynamically tuned to the temporal sequence of photon arrivals that encode natural contrast changes, typically driven by the animal's own movements.

For both types of stimulation, the signal-to-noise ratio and rate of information transfer increase with the absolute change in sampling rate; that is, the difference in the number of samples per unit time [3,31,115]. The larger the quantum-bump rate changes driving a photoreceptor's macroscopic response to a given light pattern, the higher its information transfer rate [3,31,115]. However, active visual behaviours that produce bursty, high-contrast inputs - such as saccadic eye movements and brief fixations containing rapid transients and darker intervals - drive photoreceptor encoding more effectively [3,24,27]. This advantage arises from a balanced sampling sequence: fixations on darker features relieve refractoriness and resensitise microvilli, while saccadic crossings of brighter high-contrast boundaries boost information intake by increasing quantum bump-rate changes per unit time.

This principle suggests a general rule for optimal viewing: animals should fixate on darker features [152] to recover sensitivity, then saccade across brighter regions to maximise information capture [3,24,75,153]. A young child's gaze offers a suggestive example. Newborns show a robust preference for faces, particularly their darker eye region [154,155], and as visual circuits mature, infants begin making rapid gaze shifts across brighter facial regions while extracting increasingly rich visual and social information [156].
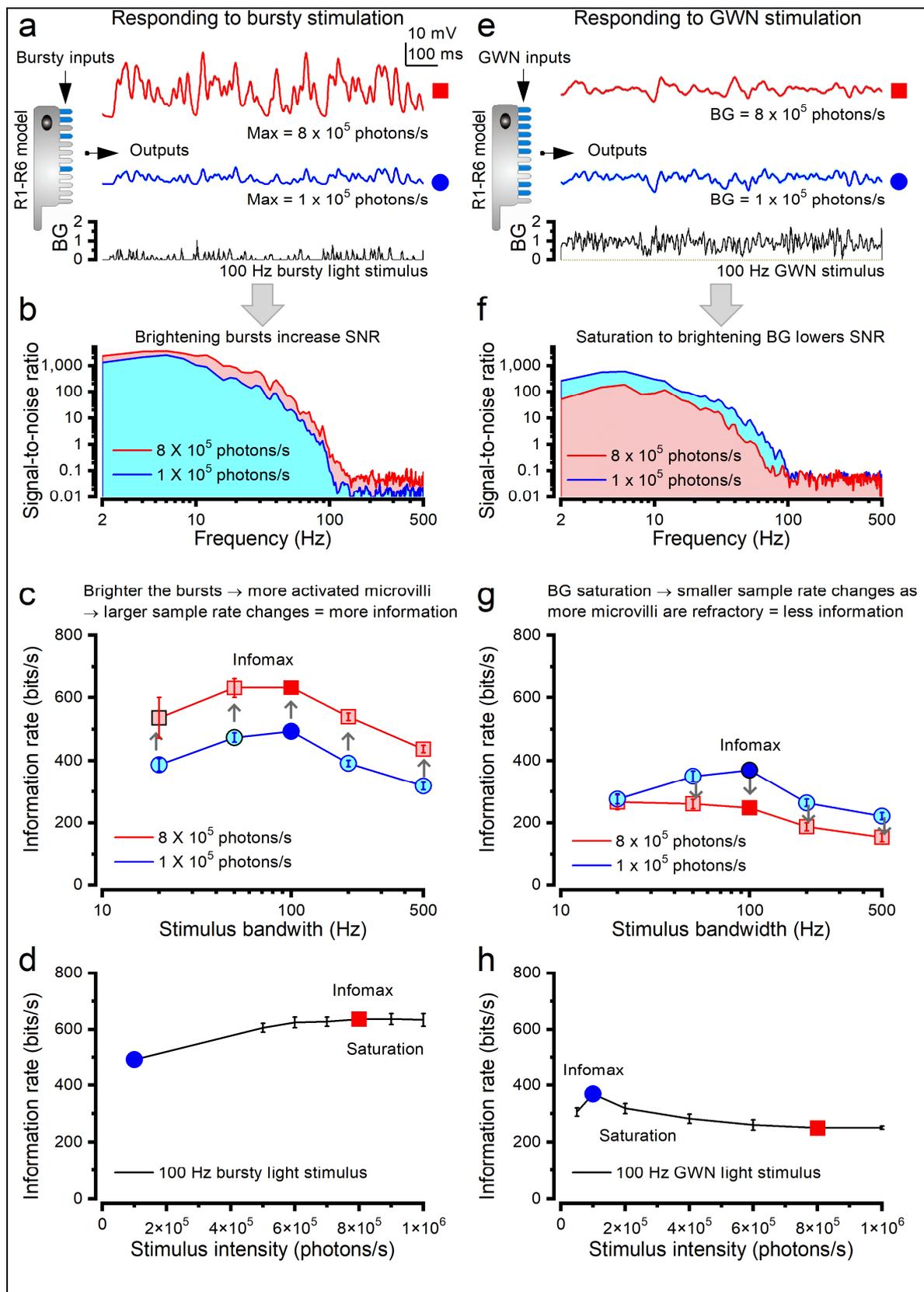
Figure 6. Refractoriness limits maximal information transfer in a *Drosophila* R1–R6 photoreceptor. Photomechanical adaptations, including the intracellular pupil [7,86] and contracting rhabdomere [23,24,26], dynamically regulate photon capture by microvilli to maximise information transfer [24]. The left panels (**a–d**) show responses to 100 Hz high-contrast saccadic bursts; the right panels (**e–h**) show those to Gaussian white-noise (GWN) stimuli [24]. (**a–d**) During saccadic bursts, dark intervals permit microvillar recovery from refractoriness, maintaining a large pool of responsive units. Brighter bursts (8×10^5 photons s^{-1} mm^{-2}, black) elicit

larger quantum-bump rate changes and, hence, larger macroscopic voltage responses than dimmer ones (10^5 photons s^{-1}, blue). (**b**) These responses exhibit higher and broader signal-to-noise ratios. (**c**) Because the bump sizes have adapted to be broadly similar for these test intensities, responses with larger bump-rate changes convey higher information rates, irrespective of stimulus bandwidth. (**d**) Information transfer increases with intensity until ~8×10^5 photons s^{-1}, when most microvilli become refractory and sampling saturates. (**e–h**) Under GWN stimulation, the higher mean light background (BG) keeps more microvilli refractory even at lower intensities. Consequently, responses to the brighter and dimmer inputs are similar in amplitude, but dimmer inputs show more high-frequency modulation (**e,f**), yielding higher signal-to-noise and information transfer (**g**). (**h**) Information transfer saturates at intensities roughly eightfold dimmer than for bursts, peaking near 10^5 photons s^{-1}. Thus, because more microvilli remain refractory during GWN (**h**) than during saccadic bursts (**d**), photoreceptors exhibit larger quantum-bump rate changes and higher information transfer during saccadic bursts. These findings indicate that photoreceptors are adapted for maximal efficiency during active, saccadic vision. Figure adapted from [24].

Quantum-bump size, if constant, does not affect information transfer rate, provided bumps are briefer than the stimulus changes they encode [32,127]. In that case, a fixed bump waveform scales signal and noise equally, consistent with the data-processing theorem [157]. However, when estimating information rates from repeated responses to the same stimulus, variability in bump size - such as its adaptive reduction during bright stimulation - is often misclassified as "noise." This apparent noise arises from the unrealistic assumption that the system is stationary and that noise is simply added to the signal at each processing stage.

This modelling framework can be extended to incorporate additional morphodynamic and structural details, making the simulations even more realistic (**Figure 4**). Simulated responses closely match intracellular recordings when measured photoreceptor microsaccade movements [24,26,27] and synaptic feedback from first-order interneurons are included [27,49,142,158], yielding a multiscale morphodynamic model of spatiotemporal visual information sampling (**Figure 4a**, **b**). Thus, intracellular photoreceptor recordings capture not only the intrinsic phototransduction response to light-contrast changes but also, to a lesser extent, modulation by superimposed synaptic feedback [27,49,79,80,158]. By circulating accumulated information among R1-R6 photoreceptors with partly overlapping receptive fields [26,27,159] (**Figure 4b**), this feedback sharpens voltage waveforms and enhances their feedforward transmission to LMCs [27,49,80,142,145] (**Figure 4e**). We return to these models at the end of Part I.

1.3.4. What Are the Benefits and Costs of Adaptive Stochastic Sampling?

Stochastic refractory quantal sampling is not only an elegant light-adaptation strategy but also a generic solution to the temporal aliasing problem. It scatters high-frequency information into broadband noise rather than producing false patterns associated with regular sampling [3,24,160]. Variable sampling times and amplitudes therefore prevent distortions or artefacts when reconstructing macroscopic responses from continuous light patterns. Likewise, the topological disorder of photoreceptors, with varying sizes and uneven positioning in the retina [161,162], provides anti-aliased sampling of spatial and chromatic information from visual scenes [3,24,26,145,160]. Intrinsic biophysical heterogeneity within neuron populations [27] can further enhance the information content and robustness of their collective spatiotemporal signalling [3].

The trade-off of stochastic sampling is broadband noise [24,160]. However, because each photoreceptor's multiple rows and columns of microvilli sample light from a common source, this spatiotemporal parallelism effectively minimises noise [32,127]. Noise is further reduced as quantum-bump amplitudes and rates adapt to ongoing stimulation, and when signals converge synaptically, as in the morphodynamic neural superposition (**Figure 4a,b**), where each LMC overcompletely samples visual information from the same small area [27,49,80].

In 1907, Sir Francis Galton showed that simple aggregate statistics, such as the mean or median of many independent estimates reported by honest observers, can provide a remarkably accurate

approximation of a witnessed event [163]. A year earlier, at a country fair in Plymouth, the crowd was asked to guess the weight of an ox. Galton analysed these estimates and found that while individual values varied widely, their median came astonishingly close to the true weight. By analogy, in fly photoreceptors, the observers are the tens of thousands of microvilli, each of which has either recently absorbed photons or not. A microvillus that captures a photon casts an independent "vote", producing a quantum bump or no bump, on how surprising that event is given its recent light history. The weighted average of these simultaneous votes, the macroscopic voltage response, yields a reliable, non-aliased and, under bright conditions, nearly noise-free dynamic estimate of the incoming light signal [3,7,24,27,31,32,127]. This estimate is tuned to the animal's visual requirements and is embedded in the morphodynamic architecture and stochastic, quantal, refractory biophysics of phototransduction.

1.3.5. Photoreceptor Structure Defines Its Encoding Performance

Photoreceptors of different species have likely evolved morphologies and properties tuned to the visual demands of their lifestyles [143]. A photoreceptor's maximum information transfer rate cannot exceed its structural limits, which are set by the total number of microvilli and their maximum quantum bump production rate [24,31], as constrained by the speed of phototransduction reaction inside microvilli and their recovery (refractoriness) (**Figure 7a**). Photoreceptors with more microvilli and faster microvillar turnover, in principle, provide better vision by serving the brain with higher information rates (right). Accordingly, the fast-flying, aerobatic housefly *Musca*, an extreme diurnal specialist, possesses more and faster microvilli than the slower, crepuscular fruit fly, *Drosophila* [7,27,31].

However, these structural advantages come at a cost: more microvilli increase the plasma membrane capacitance and thereby the membrane time constant [7,31,32]. A larger, slower time constant can only be offset by larger conductances, which ultimately require greater ATP consumption [164]. Thus, faster and larger responses are metabolically more expensive, because their ionic driving forces must be restored by ion exchangers whose work consumes energy [7].

In both species, the actual information rate that photoreceptors can achieve also depends on the structure of the visual environment and on how the flies sample it through active sensing and photoreceptor microsaccades. As explained earlier (**Figure 6**), Gaussian white noise mean-adapts photoreceptors, driving many microvilli into a refractory state. Consequently, regardless of how scanning motion moves photoreceptors across a stimulus, randomised spatial patterns such as Gaussian white noise generate smaller changes in quantum bump rate and therefore carry less information than naturalistic patterns scanned with (targeted) saccades and fixations [24]. Increasing evidence now indicates that, for the most efficient vision, saccadic scanning motion has been matched through evolution with the photoreceptors' morphodynamic stochastic quantal sampling properties [3,7,24–27,31,32].
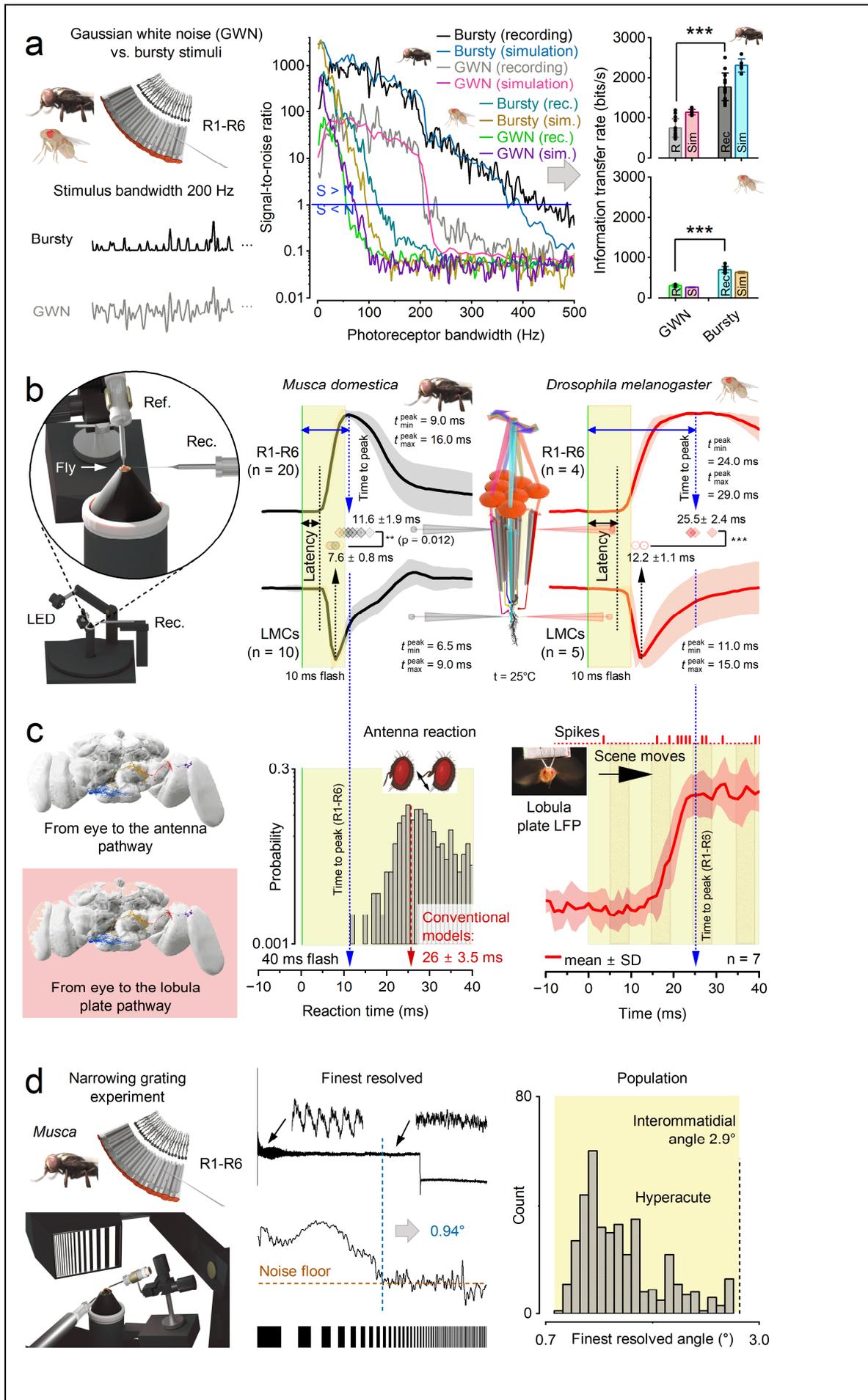
Figure 7. Fast sampling motion (saccadic scanning and photoreceptor microsaccades) synchronises and enhances visual processing and perception in flies. (**a**) Saccade-like bursty stimuli drive efficient encoding in housefly (*Musca domestica*) and fruit fly (*Drosophila melanogaster*) R1-R6 photoreceptors, but Gaussian white noise (GWN), even with twice as much power, cannot [7,24,27]. Bursty inputs contain rapid transients and darker intervals that relieve microvillar refractoriness, whereas the mean-adapting GWN keeps more microvilli refractory. Consequently, response signal-to-noise ratios (SNRs) are higher during saccadic bursts. In *Musca*, for example, responses maintain SNR > 1 up to ~440 Hz, whereas under GWN this threshold is crossed near ~210 Hz. Bursty inputs, therefore, yield substantially higher information-transfer rates. Motion-based saccade–fixation sampling thus improves photoreceptors' efficiency in translating rapid photon-rate changes into quantum-bump rate changes, increasing SNR and information throughput for behaviourally relevant visual signals. (**b**) Intracellular voltage recordings from *Musca* and *Drosophila* R1–R6 photoreceptors and their postsynaptic large monopolar cells (LMCs) [27,49,79,80]. Although LMC waveforms rise and peak much faster than photoreceptor responses, both cell types show identical response latencies from stimulus onset (~4 ms in *Musca*, ~7 ms in *Drosophila*), indicating no measurable synaptic transmission delay. LMC responses, therefore, align closely with fast visual behaviours and downstream neural processing, peaking significantly earlier than their photoreceptor inputs. (**c**) Light-evoked voluntary antennal movements in *Musca* occur in close temporal synchrony with R1–R6 photoreceptor responses [27]. The shortest reflex pathway from photoreceptors to antennal motor neurons contains six synapses spanning ~2,100 μm, yet antennal lift responses emerge only ~13–20 ms after stimulus onset, within the time window of photoreceptor peak responses (9–16 ms). In *Drosophila*, local field potentials (LFPs) and spikes recorded in the optic lobe of tethered flying flies show strong motion sensitivity, with activity emerging consistently ~10 ms after motion onset, earlier than the peak of flash-evoked photoreceptor responses. LFP traces are inverted for comparison, and all responses are amplitude-normalised. These observations show that visually guided behaviours can arise faster than conventional feedforward conduction models predict. (**d**) Photoreceptors exhibit hyperacute spatial discrimination beyond the anatomical spacing of ommatidia [24,26,27]. Left: schematic of the narrowing-grating experiment. Middle: example R1–R6 responses reveal resolvable modulation down to 0.94°, far below the interommatidial angle (2.9°). The orange dashed line marks the noise floor. Bottom: progression from coarse to fine gratings. Right: population data show that many photoreceptors resolve spatial angles <2.9°, demonstrating that morphodynamic sampling enables resolution beyond the compound eye's anatomical sampling grid.

1.4. Active Sensing Drives Both Efficient Information Sampling and Predictive Coding

To perceive the world efficiently, neural processing in the eye must adapt to environmental regularities such as the luminance structure of natural scenes [8]. Much of this adaptive capacity is genetically pre-encoded in the retinotopic sampling matrix, physical properties, and behavioural repertoire of each species [3]. These innate features shape optical design, muscle coordination, and retinal circuitry, aligning sensory architecture with the saccadic behaviours used to explore natural environments.

For example, the photomechanical photoreceptor microsaccades are approximately 2–3 times faster and smaller in *Musca* than in *Drosophila*, matching their respective eye architectures and flight speeds [24–27]. *Musca* possesses smaller interommatidial angles and performs faster turns during flight, requiring correspondingly faster photoreceptor sampling dynamics. These relationships challenge the historical view of visual computation based on static structures and sequential filter models.

In the classic static view, the eye resembles a pixelated camera that integrates snapshots during "motionless" fixations. Saccades were thought to blur these images, requiring an efference copy to suppress the blur at the sensory surface. This assumption was applied especially to flies, whose extreme angular velocities and presumed slow photoreceptor responses were believed to render them briefly "blind [165]." Yet, paradoxically, everyday experience shows the opposite: flies buzzing around your head dodge every swat with uncanny precision.

A different perspective emerges when visual sampling is considered as an active, motion-coupled process. In this dynamic view, the eye forms a morphodynamic matrix of photoreceptors

and interneurons in which rapid adaptation both generates photoreceptor microsaccades and exploits motion-induced image shifts to achieve ultrafast, high-acuity vision [24,26,27]. Evidence from insects and mammals, combining experiments and modelling, converges on the conclusion that visual sampling is most efficient during active sensing, driven by rapid saccades interspersed with brief fixations [24,26,27,71,73,74,166–168].

Flies exemplify this principle. *Musca* visual neurons achieve record rates of information sampling (~2,500 bits per second; **Figure 7a**) and synaptic transmission (~4,100 bits per second; **Figure 4e**), with LMC bandwidths extending to ~1,000 Hz. These values far exceed classical estimates of flicker-fusion frequency (~230 Hz) derived from extracellular electroretinograms [169], and imply extremely rapid synaptic signalling [27] (**Figure 7b**).

Behavioural assays reveal response latencies of only 13 to 20 ms (**Figure 7c**, middle), even while photoreceptor signals are still rising (**Figure 7b**, middle). Such rapid behavioural responses challenge sequential feedforward models based solely on conduction delays and synaptic integration. Consistent with this view, lobula plate tangential neurons in the *Drosophila* optic lobe (**Figure 7c**), located at least four synapses downstream of photoreceptors, respond to wide-field motion in near synchrony with photoreceptors and LMCs. These observations imply that early visual processing must incorporate predictive coding mechanisms.

Intracellular recordings of light-contrast bursts revealed synaptic high-frequency jumping, in which photoreceptor–interneuron synapses dynamically shift transmission toward higher frequencies during contrast bursts (**Figure 4e**), mimicking the light-change patterns generated by rapid saccades followed by brief fixations [27]. At the photoreceptor level, *Musca* photoreceptors adapt through refractory quantal sampling: ~54,000 microvilli per cell absorb 10^5-10^6 photons s^{-1} while dynamically adjusting quantum efficiency to maintain high signal-to-noise ratios [27] (**Figure 7a**). Photoreceptor microsaccades and flight saccades enhance contrast detection and maintain accurate scene estimates without saturating the neurons' encoding range. Each LMC integrates inputs from six photoreceptors (seven in the male "love spot") through partly overlapping receptive fields that shift photomechanically during stimulation. Combined with directionally tuned microsaccades, this pooling enables hyperacute pattern detection down to ~0.7°, well below the interommatidial spacing (2.9°) and even beyond the diffraction limit of an average ommatidial lens (~1.1°) [27] (1.1°) (**Figures 7d** and **4c,d**).

Importantly, synaptic high-frequency jumping emerges specifically during active saccades, but not during stimulation with Gaussian white noise or linearly scanned light patterns from the natural environment [27]. Together with photomechanical photoreceptor microsaccades, this mechanism enhances phase congruency between spatial features, allowing edges and object outlines to become rapidly detectable [27]. A biophysically realistic morphodynamic model reproduced these observations (**Figure 4e**), demonstrating how photomechanical motion, quantal sampling, synaptic dynamics, and microvillar refractoriness co-adapt with active sensing to minimise delays and maximise information transfer.

1.5. Active Sensing Adapts to the Natural Environment to Enhance Spatiotemporal Resolutions

To illustrate how morphodynamic sampling influences neural resolvability, we consider a simple example: a fly observing two nearby moving objects (**Figure 8**). Intracellular LMC recordings are compared with model predictions ranging from the full morphodynamic neural superposition model to simplified variants with progressively reduced biological detail.

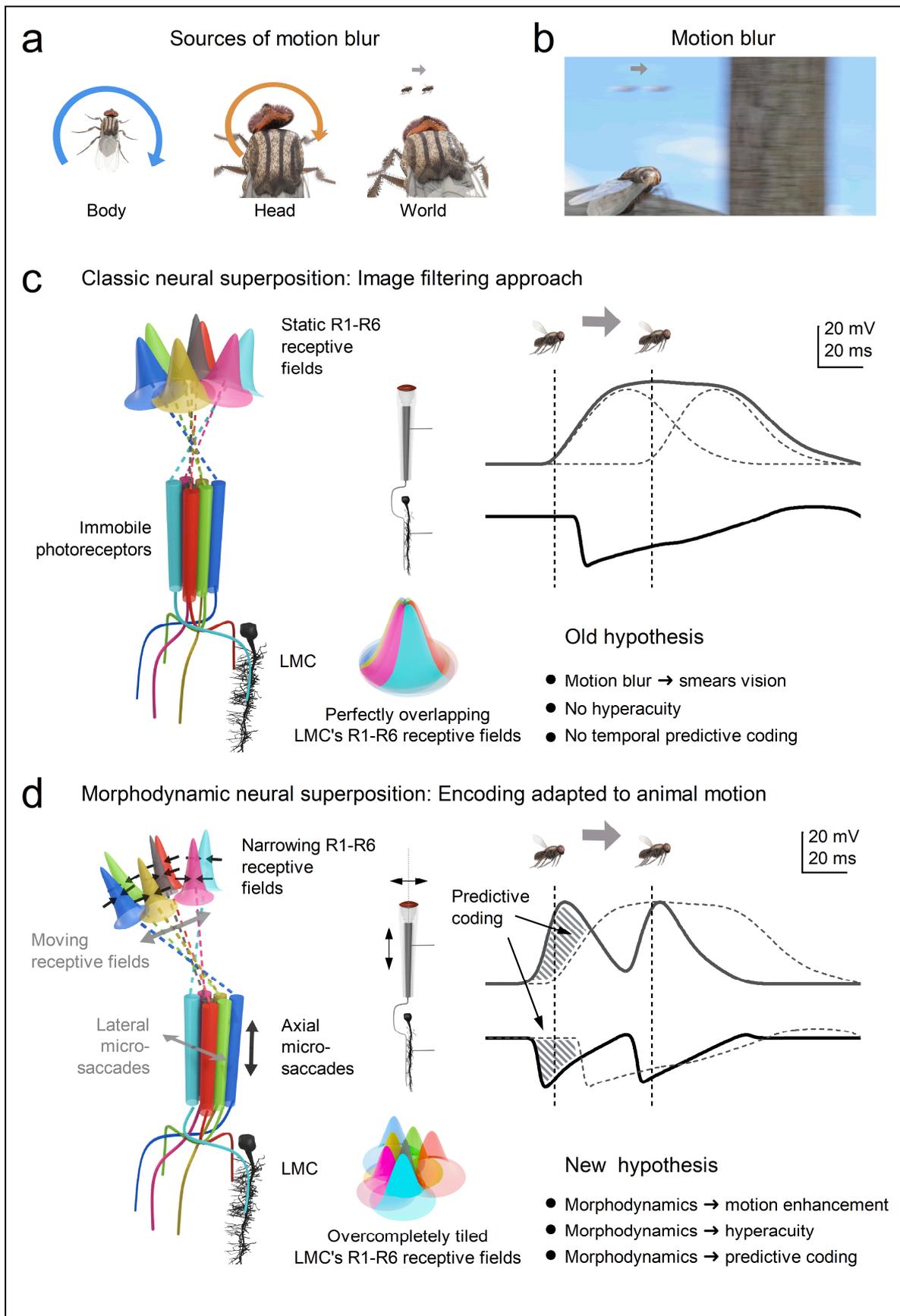**Figure 8. Morphodynamic quantal–refractory sampling and synaptic high-frequency jumping enable predictive encoding of fast-moving objects while counteracting motion blur**. The conventional static filtering model (classic neural superposition) is contrasted with the experimentally grounded morphodynamic neural superposition framework in early fly vision. (**a**) Motion-induced image shifts in natural vision. Retinal input is

continuously perturbed by rapid rotations of the body and head, as well as by fast movements in the environment. During walking or flight, these saccade-like turns generate abrupt, high-contrast image displacements on the retina, creating conditions traditionally associated with motion blur. (**b**) Classical expectation: motion blur. If retinal sampling were purely static, rapid image motion would smear spatial detail and broaden temporal responses, reducing positional accuracy and limiting discrimination of fast-moving objects. (**c**) Classic neural superposition as a static image-filtering scheme [165,170,171]. In the traditional formulation, R1–R6 photoreceptors are treated as immobile detectors with fixed receptive fields that combine via large monopolar cells (LMCs) to represent a single spatial location. The pooled LMC receptive field is depicted as a perfectly overlapping composite of equivalent photoreceptor inputs. Encoding is typically described as convolution of static spatial filters with temporally integrating impulse responses derived from noise analysis. Under these assumptions, responses to moving objects are predicted to be spatially and temporally blurred: nearby objects merge, response peaks lag stimulus position, and neither hyperacute localisation nor intrinsic phase advancement emerges from the model. Vertical dashed lines indicate when the moving object aligns with the geometric centre of the receptive fields. (**d**) Morphodynamic neural superposition: motion-adapted sampling. In the morphodynamic framework, R1-R6 photoreceptors differ systematically in axis orientation and receptive field structure, forming an overcomplete spatial mosaic [26,27,159]. Crucially, these sampling elements are dynamic rather than static. During phototransduction, ultrafast axial and lateral photomechanical microsaccades transiently shift and narrow effective receptive fields, reshaping spatial sampling in time and coupling it to self-motion. Stochastic, quantal, and refractory sampling in R1-R6 photoreceptors interacts with synaptic high-frequency jumping at the photoreceptor–LMC synapse [27]. Together, these processes are predicted sharpen spatial discrimination and reduce effective motion blur. When receptive-field motion counteracts object motion, neural responses are expected to advance relative to stimulus position, producing temporally precise, phase-leading signals (striped region). Figure adapted from [27].

Natural vision unfolds in three-dimensional environments where objects continuously appear, disappear, and occlude one another as animals move (**Figure 8a,b**). Visual systems must therefore resolve dynamic spatial structure under conditions of rapid self-motion, abrupt contrast transitions, and partial occlusion. Classical static models predict that such conditions inevitably degrade spatial precision through motion blur and temporal lag (**Figure 8c**). However, if sensory sampling itself is motion-coupled, rapid image shifts can instead provide structured temporal cues that enhance, rather than impair, resolution (**Figure 8d**).

In fly compound eyes, photomechanical microsaccades generated within individual photoreceptors dynamically shift and transiently narrow receptive fields during contrast changes. Because neighbouring photoreceptors are arranged in an overcomplete neural superposition architecture (**Figure 9**), these microscale motions transform spatial differences into precisely timed temporal signals at the level of LMCs. As moving objects emerge from behind occluding edges (**Figures 9a,b**), receptive-field clipping and morphodynamic displacement sharpen spatial sampling and synchronise neural responses with object motion [27]. Motion is therefore not merely tolerated but exploited to increase discriminability.

Electrophysiological recordings combined with parameter-free morphodynamic modelling (**Figure 9c**) show that this architecture preserves hyperacute discrimination even at saccadic velocities [27] (**Figures 9g,h**). Spatial separations well below the anatomical interommatidial spacing can be resolved, and response peaks occur with minimal delay relative to stimulus position.

Reduced model variants lacking photoreceptor microsaccades or dynamic synaptic interactions exhibit slower and more blurred responses, consistent with predictions from static filtering models (**Figures 9d-f**). These comparisons indicate that motion-coupled morphodynamic sampling is essential for maintaining spatial precision and temporal accuracy during fast behaviour.
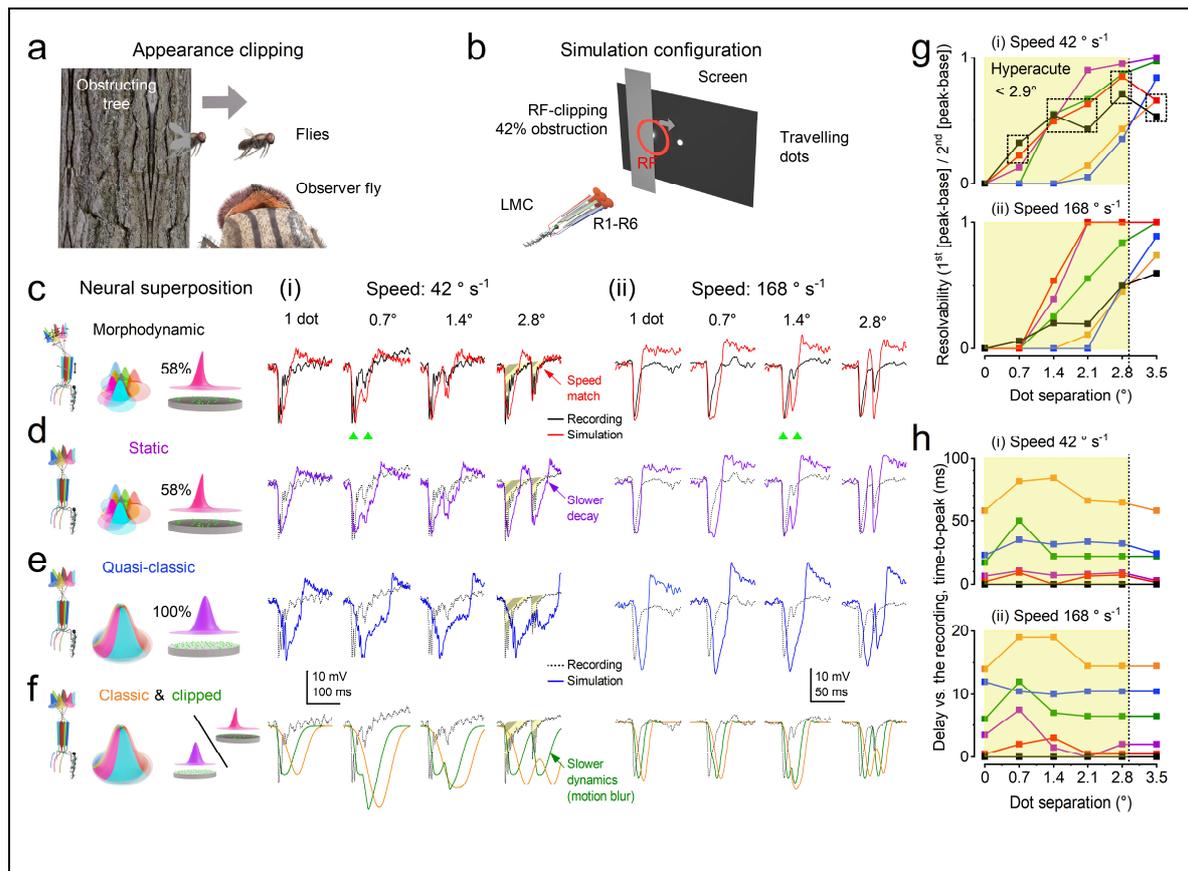
Figure 9. Motion-coupled morphodynamic sampling preserves hyperacute resolution during occlusion. Intracellular recordings from large monopolar cells (LMCs) are compared with simulations from progressively simplified neural superposition models during controlled visual stimulation in which one or two small moving dots emerge from behind a partially occluding plate. (**a**, **b**) Behavioural scenario and stimulus configuration. Moving dots appeared from behind an occluding edge positioned near the centre of the LMC receptive field, mimicking natural object emergence during self-motion. LMCs integrate inputs from R1–R6 photoreceptors. (**c–f**) Model comparison. The full morphodynamic neural superposition model (**c**) closely reproduces the ultra-brief, precisely timed phasic LMC responses observed experimentally. Removing photoreceptor microsaccades (**d**), enforcing perfectly aligned receptive fields (**e**), or reducing the system to a classical static filter model (**f**) progressively degrades temporal precision and spatial resolvability. Static formulations predict slower, blurred responses and little or no hyperacuity. Responses are shown for dot velocities of 42° s⁻¹ and 168° s⁻¹ (saccadic speed), and for separations down to 0.7°. Black traces show recordings; coloured traces show model predictions. (**g**, **h**) Quantitative comparison. The morphodynamic model matches recorded resolvability and exhibits near-zero peak delays, indicating accurate temporal alignment. It resolves separations well below the anatomical interommatidial limit (~2.9°), maintaining hyperacute discrimination even at saccadic velocities. Together, these results illustrate that motion-coupled morphodynamic sampling is required to counteract motion blur and generate predictive, low-latency encoding when objects emerge from occlusion. Figure adapted from [27].

Mechanistically, two interacting feedback loops contribute to this enhancement [27]. Photoreceptor-level microsaccades (**Figures 4b,d**) primarily sharpen spatial resolution by dynamically reshaping receptive fields, whereas the simultaneous (interlinked) synaptic feedforward and feedback dynamics [3,24,26,27,49,80,142] (**Figure 4b**) coordinate phasic transmission and redistribute power toward higher frequencies [27], supporting predictive timing. Together, these processes convert self-generated motion into a computational advantage, enabling high-resolution, low-latency encoding in cluttered and rapidly changing environments.

Flies therefore actively shape their sensory input through rapid saccades and brief fixations that drive efficient morphodynamic sampling and predictive visual processing [3,24,26,27]. Similar principles operate in vertebrate vision: even during fixation, human eyes exhibit constant

microsaccades and tremor. When these movements are artificially suppressed, visual perception fades as retinal neurons adapt to an unchanging image [152,172–174]. We therefore rely on these tiny jitters to inspect fine detail, since perfect fixation would make the scene disappear. Generalised across animals, these findings imply that saccadic behaviour, automatic and largely outside conscious awareness, maximises sensory information capture by driving efficient morphodynamic sampling. Together, these multiscale sampling movements may constitute a component of the brain's *System 1* in Kahneman's sense [175], keeping vision continuously in a state of minimal delay and high acuity.

To summarise the main message of Section I: explaining the extreme speed, dynamic range, and spatial precision of fly vision requires moving beyond purely static filter descriptions toward mechanistic accounts grounded in cellular microstructure [3,24,25,27,31]. In microvillar photoreceptors, tens of thousands of stochastic sampling units operate under refractoriness, while rapid ultrastructural motions couple mechanical displacement directly to the timing and statistics of quantal responses. Under the burst-like contrast dynamics generated during active saccades, this quantal–morphodynamic substrate naturally enhances gain control, sharpens temporal precision, and supports hyperacute spatial discrimination. Extending this framework to the first visual synapse helps resolve the apparent mismatch between classical bandwidth estimates and behavioural speed. During naturalistic contrast bursts, photoreceptor–interneuron transmission dynamically redistributes power toward higher frequencies, effectively minimising synaptic delay and enabling near-kilohertz bandwidths with information transfer rates in the thousands of bits/s.

Phenomenological filter-based or fixed-bandwidth models can often reproduce selected response statistics and have provided valuable descriptive insights into neural coding (**Figure 8c**). However, such approaches typically treat speed, dynamic range, and resolution as externally constrained parameters. In contrast, when quantal stochastic sampling and ultrastructural dynamics are embedded within naturalistic input conditions (**Figures 8d** and **9c**), these performance limits arise as coupled consequences of identified biophysical mechanisms. In this way, cellular microstructure provides a direct mechanistic substrate to behaviourally relevant neural performance. Together, these findings illustrate how active sensing and morphodynamic sampling jointly link cellular structure, synaptic dynamics, and behaviour, offering a coherent mechanistic account of efficient, predictive neural computation.

2. Section II: Global Information Representation Ties Motion to Encoding and Perception

How do insects, with tiny brains of fewer than a million neurons, short adult lifespans, often just days or weeks, and limited opportunities for learning, nonetheless develop sophisticated cognitive abilities? The world's object feature space is vastly larger than the number of neurons available to represent it, creating a fundamental mismatch between sensory inputs and neural outputs. To bridge this gap, insect brain circuits must implement space-saving, cost-efficient encoding strategies in which single neurons contribute to multiple functions. These constraints favour combinatorial, distributed representations that expand the effective encoding space far beyond the number of physical neurons.

We argue that efficient insect cognition arises because genetically scaffolded neural circuits, animated by self-generated motion, transform high-dimensional sensory inputs into distributed semantic representations of objects, while simultaneously integrating this information with motor commands and goal-oriented decision-making across the brain.

This challenge is met because the brain is not a blank-slate communication network at birth, but a genetically organised system already equipped with an internal world map that links sensing, planning, and action to specific body parts and reference frames. Its wetware is the physical embodiment of this prior structure. This innate organisation makes neural encoding predictive by design [8,176]. During development, ancestral genetic information guides the self-organisation of this world map, its basic scaffolding, and its body-centred coordinate space for perceiving and acting in environments shaped by predictable regularities [33,35,36,39,68]. Experience then continuously tunes

this system by dynamically modifying the structure–function relationships of its constituent parts [177]. Rapid, phasic neural responses, driven by morphodynamic processes and therefore hyperacute in time, further increase the dimensionality of this encoding beyond what any static network of similar size could achieve [3].

Thus, self-generated sampling motion across multiple scales continuously interacts with genetically specified neural architecture to capture sensory input. Together, these processes shape how sensory information is sampled and organised within retinotopic and body-centric feature maps distributed across the functional connectome. This integrated scaffolding binds sensory and motor signals with decision-making at a global level, supporting perception and enabling sophisticated behaviours, such as hyperacute stereovision in insects [26]. We propose that active sensing, together with the interplay of morphodynamic, electrical, and chemical processes, animates the brain's internal representations of the world. Through this dynamic structure–function interaction, perception continuously reshapes neural landscapes while preserving the capacity for complex cognition and adaptive learning. Embryogenesis, directed by ancestral gene networks, establishes the brain's initial form and functional organisation, creating maps of external regularities that are subsequently refined through experience - effectively a virtual-reality-like learning process in which self-generated actions shape sensory input. Thus, when a calf is born, it can already locate its mother, and within minutes, walk to her, and begin suckling.

2.1. Genetic Scaffolding and Active Sensing Enable Semantic Encoding

Taken together, these principles imply that higher-order neural processing is less concerned with transmitting raw Shannon information, measured in bits of unpredictable signals, and more with interpreting and integrating semantic information, the meaning of signals in the context of the organism's expectations, memories, and behavioural goals. This distinction marks a shift from viewing the brain as a channel for transmitting signals to viewing it as a system for interpreting meaning. Thus, while Shannon information remains essential for quantifying variability at the sensory periphery, deeper brain circuits operate primarily in the semantic domain, linking new inputs to pre-existing internal representations of objects, relations, and events.
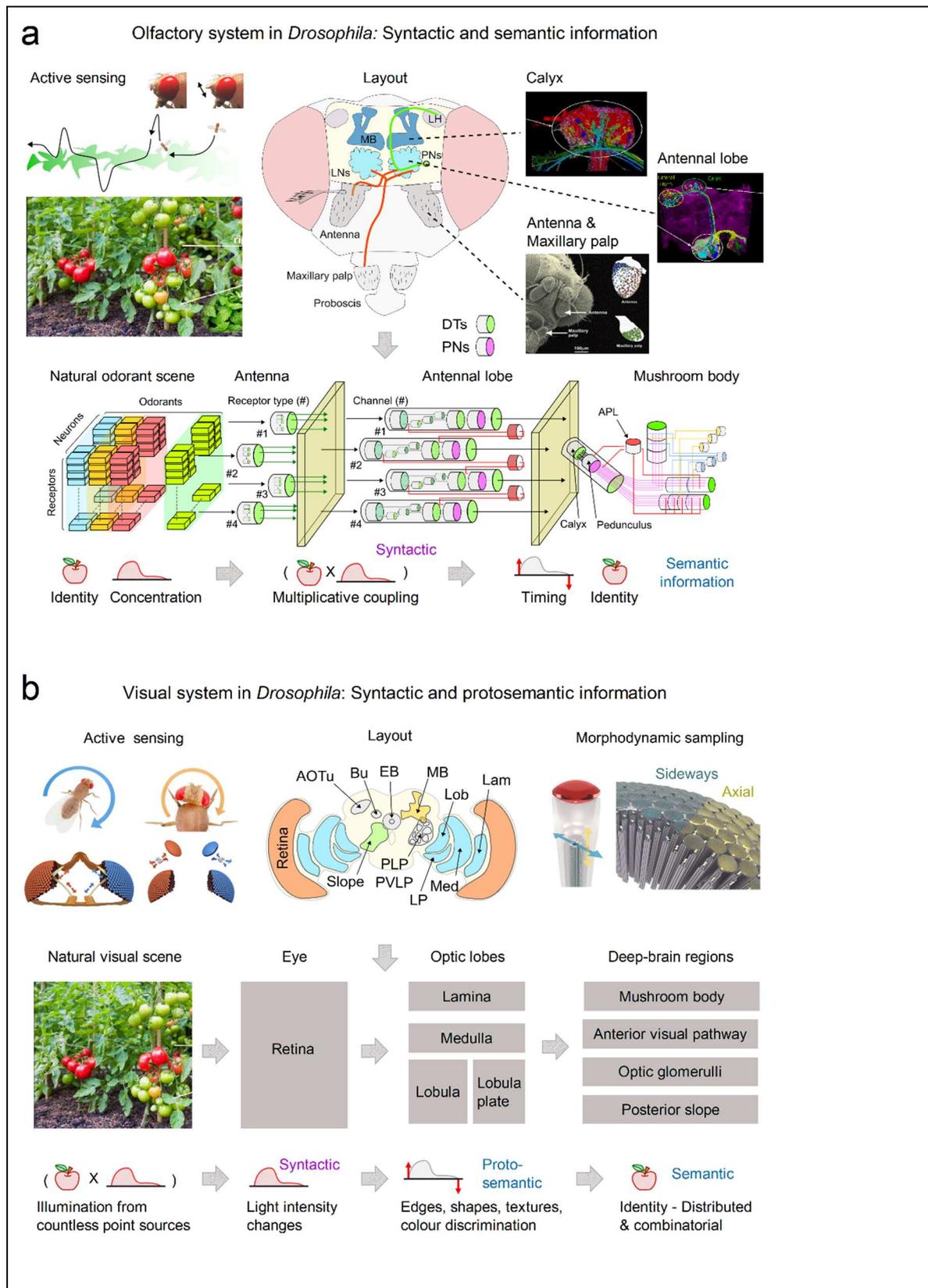
Figure 10. Syntactic, protosemantic, and semantic information processing in the *Drosophila* olfactory and visual systems. (**a**) *Olfactory system: from syntactic to semantic information*. Odour-guided behaviour in *Drosophila* arises through active sensing, in which stereotyped locomotor strategies (crosswind casting and upwind surging) interact with turbulent odour plumes to structure sensory input in time [178–180]. Natural odour scenes consist of multiple odorants with varying identities and concentrations. At the antennae and maxillary palps, olfactory receptor neurons (ORNs) expressing distinct receptor types sample this high-dimensional chemical space. Their responses encode both odorant identity and concentration through receptor-specific activation

patterns [65,181,182]. In the antennal lobe, convergent ORN inputs are reorganised into parallel glomerular channels, where local circuitry transforms receptor signals into temporally structured population responses. Here, odorant identity is multiplicatively coupled to concentration-dependent temporal dynamics, producing a syntactic neural code in which timing, gain, and relative activation across channels carry information. Downstream, in the mushroom body calyx and pedunculus, with APL neuron (Anterior Paired Lateral) modulation, sparse and decorrelated representations integrate across channels to generate semantic information - object-like odour identities that are largely invariant to concentration and suitable for learning, memory, and decision-making. (**b**) *Visual system: from syntactic to protosemantic and semantic information*. Visual perception likewise depends on active sensing, mediated by saccadic body, head, and retinal movements, as well as photoreceptors' photomechanical morphodynamic sampling, that structure incoming light signals. Natural visual scenes are composed of illumination from countless point sources and exhibit strong spatial correlations. At the retina, photoreceptors transduce these inputs into local light-intensity changes, generating a syntactic code dominated by contrast and temporal modulation [24,27]. In the optic lobes (lamina, medulla, lobula, and lobula plate), successive circuit layers extract increasingly complex visual features [168,183,184] - edges, motion, colour, textures, and shapes - forming protosemantic representations that correspond to reusable visual primitives rather than full object identity. These feature representations are then distributed to deep-brain regions, including the mushroom body and anterior visual pathways, where they are combined across space, time, and modality into semantic representations of objects and scenes. Visual object identity thus emerges as a distributed, combinatorial code shaped by circuit architecture, active sensing, and behavioural context. AOTu - Anterior Optic Tubercle; Bu - Bulb (a component of the lateral complex); EB - Ellipsoid Body (a component of the central complex); MB - Mushroom Body; Lob - Lobula (a part of the optic lobe); Lam - Lamina (a part of the optic lobe); PLP - Posterior Lateral Protocerebrum; PVLP - Posterior Ventrolateral Protocerebrum; PL - Pars Lateralis (a neuroendocrine centre); Med - Medulla (a part of the optic lobe).

In the sensory systems, this transition begins already close to the edge, at the periphery, just after the stage of morphodynamic quantal refractory information sampling, which maximises sensory (syntactic Shannon) information. For example, in the early olfactory pathway, the major challenge after sampling a fluctuating stream of quantal odorant information is to determine how an odorant object (e.g., the smell of a rose) can be reliably identified despite variations in the concentration amplitude of odorant molecules within the odorant plume. As in vision, this sensing is active and strongly phasic. Mammals, typically, sniff or perform specialised movements, such as horses curling the upper lip (Flehmen response), to enhance detection and encoding [185–190]. Insects actively move their antennae toward areas of higher odour concentration to track a scent trail.

2.2. Shared Design Principles for Representing Semantic/Syntactic Sensory Information

Drosophila olfactory circuits (**Figure 10a**) sense and process a wide range of information streams arising in many environmental niches. The odorant spaces associated with these niches contain, among others, identifiable objects of interest. The early olfactory sensory system evolved to identify and characterise in detail the object features of their respective sensory world. But what is the structure, and what are the identifiable objects in these spaces? To what extent are these objects similar and/or different? Formally characterising the (i) objects of interest in the olfactory space of *Drosophila*'s natural sensory world, and the (ii) functional logic underlying the extraction of the object features, are major challenges in neuroscience.

To provide a formal characterisation of olfactory objects of interest, the semantics and syntactics of pure odorants are explicitly and separately modelled. The semantic information refers to the odorant object identity [65], and is modelled as a pair of tensors describing the binding and dissociation rates between different odorants and odorant receptors. The syntactic information is modelled as a temporal signal characterised by its odorant concentration waveform. This led to the insight that the early olfactory system of the fruit fly encodes the odorant object identity (semantic information) and the odorant concentration waveform (syntactic information) into a combinatorial neural code [182].

In accordance with Shannon's distinction between syntax and semantics [1], it has been pointed out that the traditional application of methods of information theory, signal processing and control theory to odour signal processing lacks the notion of "meaning" or semantics [65,182]. An example illustrates this point. If a neuroscientist applies a pure odorant, such as acetone, to the antennae of a fruit fly and provides only the resulting single olfactory sensory neuron (OSN) spike recordings to another neuroscientist without revealing the odorant identity, the recordings alone provide no direct clue that the stimulus was acetone. This is because different combinations of odorant identity and concentration can produce indistinguishable OSN spike trains, making the underlying stimulus identity unrecoverable without additional circuit-level processing [181]. This ambiguity reflects the ***principle of univariance***, whereby a receptor's response confounds stimulus identity with stimulus intensity. The same principle underlies classical theories of trichromatic colour vision [191,192], in which the responses of individual photoreceptors cannot uniquely determine wavelength without comparing signals across multiple receptor types.

Most experiments in the olfactory literature assume that odorant identity is known a priori. Consequently, previous approaches [193–195] have largely focused on representing syntactic information (for example, concentration amplitude), rather than addressing the computational problem of recovering odorant identity itself. Without a formal computational or theoretical framework for odorant identity, such approaches cannot serve as complete baseline models of olfactory processing. In contrast, we argue that signal processing in the early olfactory system (EOS) of the fruit fly is primarily concerned with extracting semantic information, namely odorant identity. From this perspective, olfactory research should move beyond analysing only syntactic (Shannon) information toward understanding how neural circuits transform sensory signals into representations of odorant identity.

To that end, it has been established that the Antennal Lobe and Calyx jointly remove the concentration dependency of the odorant information [65,193] from the confounding representation of the Antenna [182]. These circuits separate the odorant semantics from syntax, thereby undoing the multiplicative coupling of these two information streams in the Antenna.

The visual system in *Drosophila* faces a strikingly similar computational problem (**Figure 10b**). Photoreceptor outputs to the lamina and medulla intermingle proto-semantic features of the visual scene - such as edges, textures, colour, and object outlines - with syntactic variables including luminance levels and contrast amplitudes. As in olfaction, early visual circuits must disentangle object identity from raw signal amplitude through distributed and adaptive processing.

Because visual objects and environments generate complex, dynamically changing signals, the resulting spatiotemporal encoding is distributed across neural populations in a combinatorial manner. Through parallel synaptic processing, signal integration, and circuit-level computations, the optic lobes progressively assemble neurally consistent object representations that become increasingly distributed in deeper brain regions. These combinatorial representations bind features such as colour, shape, texture, and brightness while preserving their precise temporal relationships within the sensorimotor loop. At the same time, the retinotopic organisation of the visual system preserves information about object location and motion direction.

We suggest that local and global synchrony across visual networks may be driven partly by intrinsic morphodynamic mechanisms with thresholding dynamics, such as synaptic high-frequency jumping, which are engaged during active sensing through rapid eye movements [27].

Collectively, these systems exemplify a shared design principle: conflated sensory inputs are transformed into robust, object-centred semantic codes. These representations are punctuated by precise temporal markers that signal environmental change. Analogous to edge-computing architectures, sensory interneurons perform local, predictive computations that convert stochastic physical inputs into structured, meaning-bearing codes with minimal delay, enabling near-instantaneous communication with higher centres through a shared, consistent semantic framework.

Information sampling and processing in both the early olfactory and visual systems are most efficient during bursty input patterns [3,24,26,27,185–190], such as those generated by targeted fast

saccades followed by brief fixations in active sensing [71,72,74,76,196,197] (**Figures 2e** and **4e**). These stimulus contrast dynamics drive synaptic high-frequency jumping that minimises transmission delays and enhances ultrafast morphodynamic interactions between neighbouring neurons that support predictive coding (**Figures 4**, **7** and **8**). Collectively, these findings suggest that self-motion-enhanced edge computing has co-evolved with rapid sensorimotor feedback from the brain. This edge-computing framework integrates neural morphodynamics, specialised parallel communication channels in the connectome, and active sensing to address the binding problem at both local and global scales. As a result, these processes are expected to drive predictive sensing by enabling synchronous, network-wide semantic representations of environmental objects. These representations encode object location in x, y, and z coordinates, referenced to the animal's body-centred frame of reference and time-locked to its ongoing actions.

From this perspective, the form-function relationships of the insect central complex [198–210] (navigation) and mushroom body [168,195,209,211–215] (visual learning) circuits can be viewed as physical embodiments of the algorithms they execute. Genetic information may define the brain networks' x–y coordinates of visual space. Binocular timing differences then provide z-depth and size information, expressed as a neural activity pattern. These timing differences arise from mirror-symmetric photoreceptor microsaccades in the left and right eyes, such that right-eye microsaccades move with objects moving leftward, while left-eye microsaccades move against them [24–26]. As the object moves, the activity pattern shifts phasically in synchrony with it. Morphodynamic processes preserve high spatiotemporal resolution and maintain representations that are both generalisable and associable. Similar objects thus evoke similar activity patterns, whereas distinct objects evoke divergent patterns - akin to Kohonen's self-organising maps or the colour representations of macaque visual area V4 [42,45,46]. Central complex circuits encode object position and orientation ("Where"), while mushroom body circuits encode chromatic and contextual features ("What"). Yet, the synchronous morphodynamic activity spanning from the optic lobes to these central circuits remains largely unexplored.

To make these complex multiscale concepts tangible, we next explore real examples from powerful interdisciplinary approaches that illustrate how morphodynamic neural biophysics are matched with active sensing to enhance information capture and transfer for predictive vision.

2.3. Active Sensing Enables Efficient Extraction of Phasic Information from Natural Images in Time

Evidence from humans and insects converges on a coherent framework. Active sensing, through fixational and saccadic eye movements (**Figure 11a–d**) and through head and body movements in insects (**Figure 11e**), is not merely a mechanism to prevent image fading or a source of noise. Instead, it is an essential process that transforms the spatial luminance structure of the environment into a temporal neural code efficiently processed by the eye [24,26,27,72,74,75,126,166,216–218] (**Figures 11** and **4**).

Natural scenes exhibit 1/f spatial statistics (**Figure 11b**), meaning that neighbouring pixels are highly correlated and therefore redundant [8,107]. The small, incessant eye movements between saccades - fixational drifts and microsaccades (**Figure 11c, d**) - break this redundancy by converting static spatial correlations into temporal modulations at the photoreceptor level. Through morphodynamic, stochastic, refractory quantal sampling of photons, this temporal reformatting discards predictable correlations while amplifying informative transients, as demonstrated in *Drosophila* early vision (**Figures 4–9**), thereby reducing redundancy before cortical processing. At the same time, these eye-induced transients are expected to accelerate synaptic transmission and synchronise neural responses to specific image features [27], thereby enhancing fine-detail discrimination and initiating feature extraction directly from photoreceptor input.

Larger movements, such as saccades, generate stronger transients that complement the finer-scale drifts (**Figure 11d**), together forming a continuous sensorimotor strategy for representing space through time. Thus, rather than passively encoding images, the retina operates as an active, behaviourally coupled processor whose input statistics are shaped by its own motion. This active-

sensing framework challenges conventional feedforward models of vision. It proposes that perception arises from dynamic sensorimotor coordination, in which eye movements are integral to encoding rather than merely stabilising visual information. We expect this motion-based strategy of sampling space in time to maximise encoding efficiency and minimise transmission delays (**Figures 4–9**). The resulting high-precision flow of syntactic Shannon information at the sensory edge can then be used to update the semantic where-what-how information of the combinatorial, distributed neural object representations in real time, and to adapt sampling behaviour in a closed loop for optimal resolution. In this view, perception emerges from active sampling: a dynamic sensorimotor process that maximises information efficiency [24,27], minimises latency [27], and continuously aligns syntactic and semantic representations of the world.
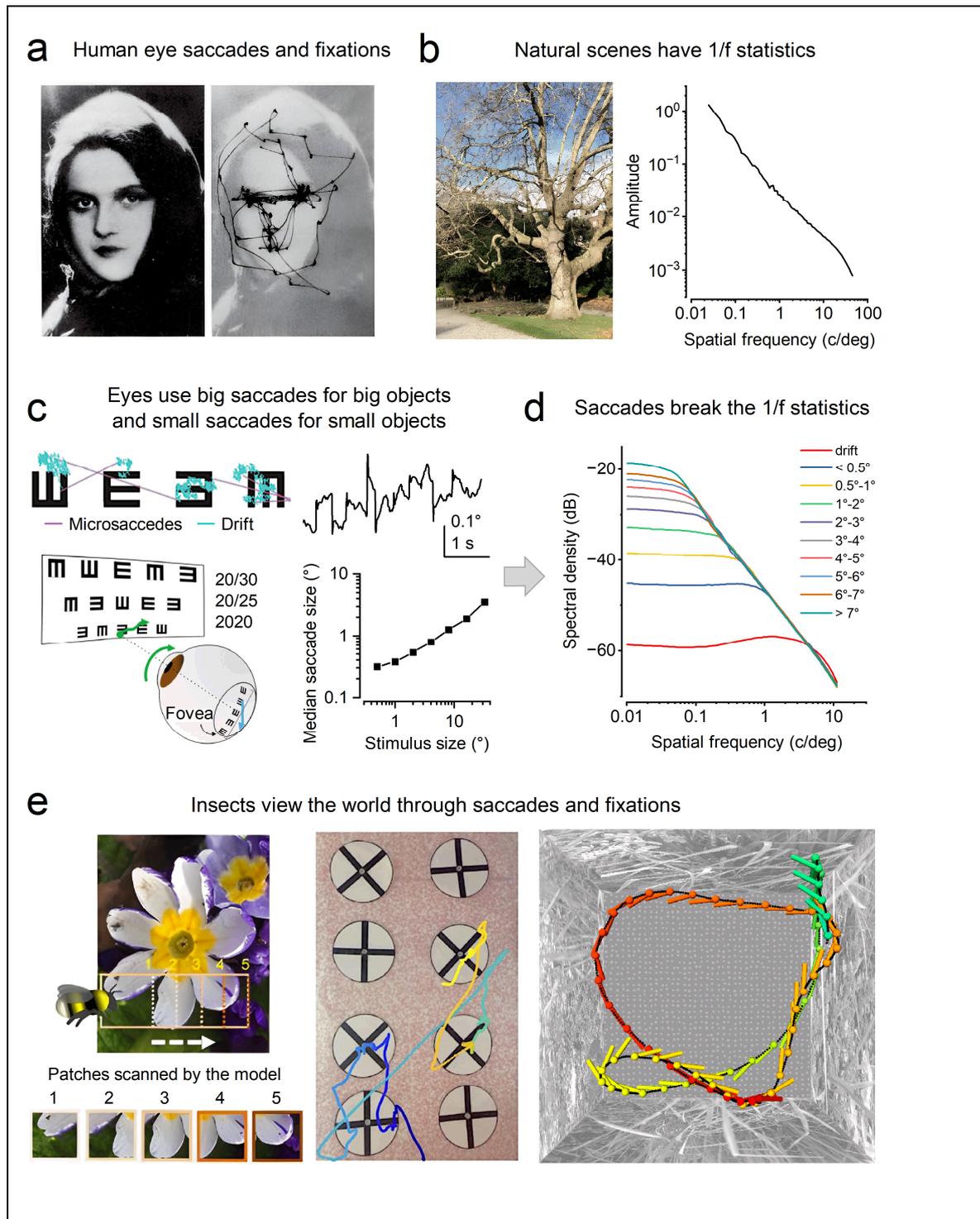
Figure 11. Human and insect eye movements likely drive efficient encoding. Microsaccades, drifts, saccades, and fixations break the 1/f image statistic [24,71–76,196,197,216,219–221], enabling the visual system to resolve objects better: transforming spatial luminance structure into bursty temporal modulations that early visual neurons are exquisitely sensitive to [24,27,222] (cf. **Figures 4-7**). (**a**) Human saccadic behaviour. Left: a classic image used in early eye-movement studies. Right: superimposed scan paths showing large saccades interspersed with fixations and microsaccades, revealing how the human visual system samples informative regions of a scene [152]. (**b**) Natural images exhibit scale-free 1/f statistics [223]. Left: example outdoor scene. Right: its spatial-frequency spectrum, which drops approximately as 1/f, indicating that low spatial frequencies dominate natural visual input unless actively decorrelated by eye movements. (**c**) Saccade size scales with object size [72,74,75,220,224]. Top left: human eyes use large saccades for large objects and small saccades/microsaccades for fine details. Top right: example eye-movement trace showing small fixational saccades during inspection. Bottom: saccade amplitude increases systematically with stimulus extent, demonstrating adaptive, object-dependent sampling. (**d**) Saccades, microsaccades and drifts transform natural 1/f input [196,216,221]. The spectral density of visual input under different eye-movement amplitudes shows a progressive flattening of the natural 1/f distribution: small drifts preferentially disrupt the fine-scale (high-frequency) portion of the spectrum, whereas larger saccades successively break coarser (low-frequency) structure. Together, drifts and saccades of adaptive sizes whiten the frequency representation of 1/f natural images, enhancing edges and local contrast and thereby driving efficient encoding. (**e**) Insects also view the world through saccades and fixations [166,168]. Left: a scanning bee sampling flower patches. Middle: model-based reconstruction of how saccade–fixate sequences segment scenes into informative subregions. Right: example flying-fly trajectory consisting of rapid saccadic turns and short fixations [110,118,222], demonstrating that insects, as in humans, use active, discontinuous sampling to sharpen spatial structure, driving efficient visual processing.

These expectations are borne out by behavioural work on active vision in bees (**Figure 11e**, left and middle) and flies (right), which provides a concrete example of how animals use self-motion to turn spatial structure into efficient temporal codes. In a pattern-discrimination task (middle), bees were asked to distinguish a multiplication sign from its 45°-rotated variant, a plus sign. Rather than distributing their gaze evenly across the whole pattern, bees executed highly stereotyped scanning flights, decelerating and hovering close to a small, task-relevant region of each stimulus before making a choice [166]. They preferentially sampled lower and lateral portions of the pattern and showed consistent left–right biases, reminiscent of task-dependent scan paths in primate and human eye movements [152,220,225–228] (**Figure 11a**).

Similar strategies were previously observed when bumblebees solved numerosity tasks: rather than "subitising" small numbers, they sequentially scanned and motor-tagged individual items, with almost no re-inspection, indicating a strong reliance on ordered, active sampling and working memory to support apparently sophisticated numerical judgements [212,229]. Crucially, in the pattern task, when only partial cues were available, bees maintained both their characteristic scanning trajectories and high decision accuracy [166]. This indicates that the actively selected glimpses already carried an abstract, object-centred representation (**Figure 11e**, middle: "plus" vs "multiplication"), robust to occlusion and context. In other words, the bees' body and head movements segmented the task into short sequences of local edge and orientation samples, converting the static patterns into temporally modulated input that can be efficiently processed by downstream circuits, paralleling the role of miniature eye movements in vertebrate vision [118,196,220,224] and of saccadic head and thorax movements in flies and other insects [230,231].

A neuromorphic model of bee active vision (**Figure 12a-d**) shows how motion-structured inputs can be transformed into compact neural codes in the optic lobe and beyond [168]. When model bees perform naturalistic scanning over image sequences, it is the self-generated motion rather than the static image content that drives non-associative plasticity in a lobula-inspired network. This learning produces spatiotemporal receptive fields jointly tuned to orientation, motion direction and speed, with sparse, decorrelated responses to orthogonal bar movements [168]. The resulting organisation matches long-standing predictions from efficient-coding and natural image statistics theories

[8,176,232,233], but is now grounded explicitly in the statistics of actively sampled scenes. Optimal decorrelation and feature selectivity only emerge when inputs are shaped by behaviourally generated movement, not under passive viewing of the same spatial patterns [168].
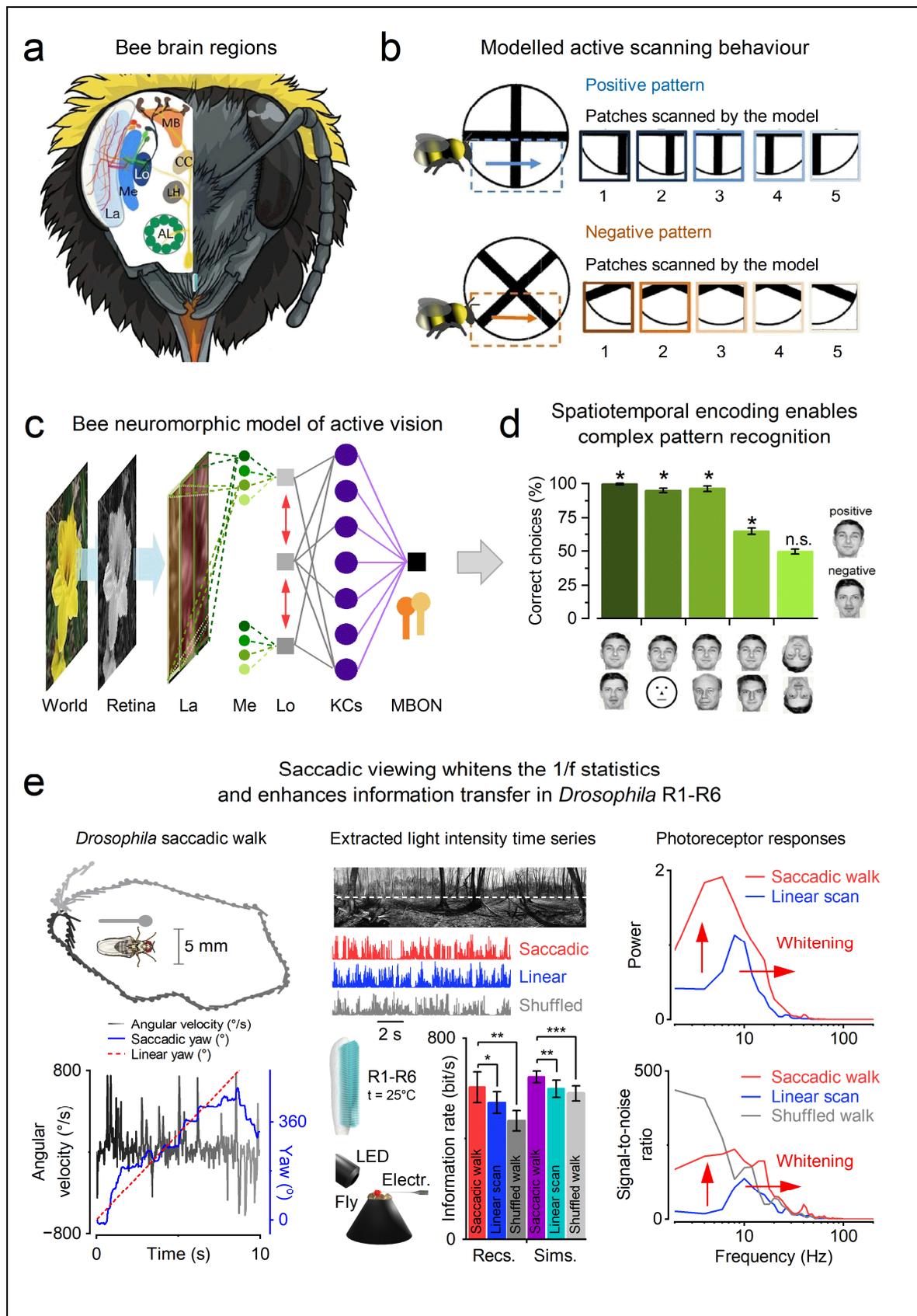

Figure 12. Active saccadic scanning of natural environments and images improves encoding, perception, and decision-making in insects and in neuromorphic models of insect vision. (**a**) Bee brain regions relevant to

active vision and learning. Schematic of the honeybee brain showing the major visual-processing centres: the lamina (La), medulla (Me), and lobula (Lo), which provide inputs to higher-order structures including the mushroom bodies (MB), lateral horn (LH) and central complex (CC). These circuits underlie visuomotor control, associative learning, and pattern recognition [168]. (**b**) Modelled active scanning behaviour promotes discrimination between similar patterns. A computational bee model performs saccade-like scanning across visual stimuli. Distinct scanning trajectories emerge for positive (blue) and negative (orange) patterns: the model samples informative patches sequentially (1–5), enabling it to extract diagnostic features from images that would be ambiguous under static viewing. (**c**) Neuromorphic model of bee active vision: spatiotemporal encoding across visual lobes and mushroom bodies. Natural scenes are first filtered by the retina and lamina, then processed through medulla and lobula circuits implemented as weighted (W) spatiotemporal filters. Output reaches Kenyon cells via sparse expansion (S) and is integrated by mushroom body output neurons (MBONs) using decision weights (D). Reward-based learning modifies synaptic parameters (Q), enabling robust discrimination even when patterns differ subtly in space or time [168]. (**d**) Active, spatiotemporal encoding enables complex pattern recognition in a neuromorphic bee model, matching behavioural results [168]. The model successfully recognises face-like patterns and other biologically relevant stimuli with high accuracy when allowed to scan images dynamically. Performance is significantly above chance for all positive patterns (*$p <$ 0.05), whereas negative patterns remain difficult to classify (n.s.). Example stimuli shown below each bar illustrate the categories tested. (**e**) Saccadic viewing enhances information transfer in *Drosophila* photoreceptors [24]. Left, above: Example walking trajectory showing rapid saccadic turns. Left, below: Angular velocity traces separating saccadic (blue) and linear (red) yaw components. Middle, above: A natural image and the corresponding light-intensity time series sampled along the dotted path using saccadic (red), linear (blue), or shuffled (grey) scanning. Middle, below: Information transfer rates of intracellularly recorded R1–R6 photoreceptor voltage responses and a biophysically realistic stochastic quantal refractory sampling model driven by the same three stimuli. Both recordings and simulations show that saccadic scanning markedly increases information rates (bits/s) compared with linear or shuffled scanning of identical images. Right, above: Linear scanning preserves the 1/f statistics of natural images, limiting high-frequency enhancement in photoreceptor responses. In contrast, during saccadic sampling, fixation periods preferentially fall on darker regions of natural scenes (reflectance <50%), allowing microvilli to recover from refractoriness. This recovery increases quantum-bump rate modulation during subsequent saccades, generating bursty responses that whiten the photoreceptor power spectrum and broaden signal-to-noise ratios (below). Together, these results show that insects exploit fast sampling movements to transform natural visual input into temporally informative signals optimised for rapid perception and action.

Complementary work on honey bees shows that these actively acquired visual features feed into compact decision circuits that dynamically adjust evidence thresholds over time, allowing animals to make fast yet accurate acceptance and rejection decisions in a manner that rivals primates and aligns with normative models of evidence accumulation and time-varying decision boundaries [234–240]. When we couple the lobula code to a mushroom body-like readout, the model solves the same pattern-recognition tasks as real bees using only the short glimpses gathered during scanning, and it generalises robustly to novel viewpoints and partial cues [166,168]. Both bees and the neuromorphic model learn, via saccadic viewing, to distinguish even human faces (**Figure 12d**).

Saccadic viewing of 1/f natural images converts slowly varying spatial luminance structure into bursty temporal sequences, transforming vision from passive information sampling to active perception. In *Drosophila*, photoreceptors encode these saccade-generated luminance transients far more efficiently than equivalent linear or shuffled scans of the same images [24] (**Figure 12e**). This improvement arises from stochastic quantal refractory sampling, constrained by phototransduction morphodynamics in the microvilli, which selectively amplifies transient changes while suppressing predictable correlations. By imposing jumpy, variable-amplitude temporal modulations on otherwise 1/f spatial inputs, saccades and fixations effectively break the redundancy imposed by 1/f image statistics. Together with quantal refractory sampling (**Figure 6a**) and synaptic high-frequency

jumping [27] (**Figures 4e** and **9**), this process whitens the temporal frequency structure (**Figure 12e**, right), generating phasic neural responses with high signal-to-noise ratios to salient objects.

Specifically, linear scanning preserves the 1/f statistics of natural scenes, limiting high-frequency enhancement in photoreceptor voltage responses (**Figure 12e**, blue trace). In contrast, because natural images contain more dark than bright regions [103,119,241] (the visible world contains more shadows and occlusions than light sources, with an average reflectance <50%), fixation periods during saccadic viewing preferentially fall on darker objects, even when fixations are imposed experimentally rather than actively selected by the animal (using previously collected behavioural data [242], as was the case here [24]). These dark fixations allow microvilli to recover from refractoriness, increasing quantum-bump rate changes during subsequent saccades [3,24]. As a result, stochastic quantal refractory sampling during saccadic eye movements and fixations (**Figure 11**) both enhances and whitens the photoreceptor signal-to-noise ratio, increasing encoding efficiency.

This tight behavioural–biophysical matching enhances information capture and transfer for predictive vision (**Figures 4e**, **7b-c**, **8** and **9**). Thus, saccades and fixations in natural environments generate the bursty luminance modulations required for efficient, minimal-delay neural processing, synchronising early photoreceptor encoding with downstream circuit dynamics that ultimately support object discrimination and decision-making.

Together, the behavioural, intracellular electrophysiology, modelling, and decision-making results demonstrate a full morphodynamic pipeline from self-generated motion at the sensory edge to distributed, object-centred representations in higher-order circuits. They show that active sensing does not merely prevent image fading. Instead, it sculpts neural population codes into sparse, invariant, "about-something" representations that are already close to the semantic object codes required for naming and recall, and in social insects for communicative behaviours such as the bee dance discussed next [243–245].

2.4. Multiscale Motion in Neural Code – A Foundation for Biological Language

If brain networks operate on semantic object representations, naming, storing, and recalling objects while continuously updating these representations through goal-directed behaviour, then these interactions naturally constitute an internal biological language model. This model relies on a shared, biophysically constrained neural code or syntax. Here, "language" does not refer to symbolic grammar or human words, but to a structured neural syntax for representing and transforming meaning.

In this view, patterns of neural activity function like words, and their separation by silent periods forms sentences. This structure mirrors the bursty organisation of neural communication, which emerges from morphodynamic, refractory, quantal transmission and sampling during active behaviours such as saccades. Importantly, these burst-based temporal relationships are scale-invariant: the same organisational principles are preserved whether neurons sample and transmit information slowly or at ultrafast rates [3,80,115]. Thus, the language is already embedded in the neural code itself, directly linking structure to function. Because brains of the same species share this internal code through their genetic architecture, they also share a common biological vocabulary. It is therefore unsurprising that animals such as bees exhibit goal-oriented, highly structured social communication, such as the bee waggle dance [243], because their brains already operate in a semantic regime.

Recent findings further show that bees use active antennal searching, or "pointing to listen," to track a dancing bee during the waggle dance [245]. Information about nectar location is therefore likely communicated simultaneously through structured vibrational motion patterns that carry a unifying multisensory code. This shared code reduces uncertainty by making information accessible not only through direct tactile interaction but also through vibrations transmitted through the honeycomb and the air, detectable by nearby hive mates at a distance.

A closely related principle is evident in the male *Drosophila* courtship "dance," a complex, genetically programmed sequence of movements and sounds [246,247]. Males chase females and

vibrate a single wing to produce a species-specific courtship song that advertises both species identity and fitness. This display is not a fixed script, but a dynamic process that integrates multiple sensory cues from the female in real time, including visual, chemical, and auditory signals. The female evaluates the male's performance by assessing song structure, timing, and pheromonal cues. A receptive female slows and pauses her movements, eventually to allow copulation, whereas an unreceptive female actively rejects the male through kicking, wing flicking, or rapid escape.

Language, in this biological sense, necessarily involves motor action. To transmit thoughts, animals must act: they speak, sing, gesture, tap, write, or otherwise shape physical signals for others to see, hear, touch, and interpret. Human language similarly depends on vocalisation, produced by precisely controlled, bursty movements of the vocal apparatus. In all cases, the intensity and temporal structure of movement are neurally tuned in a closed loop with active sensing by the sender to maximise transmission efficiency and minimise ambiguity. Thus, language in its most fundamental form emerges from active, multiscale neural dynamics rather than from abstract symbol manipulation alone.

2.5. Dimensionality Expansion in Brain Network Sampling Matrices and Resolution Limits

Motion expands the dimensionality of neural computation. Inside a neuron, molecules do not behave like tidy, isolated pieces from a textbook. Instead, they form crowded, interactive networks that are constantly in motion, assembling and dismantling subcellular structures. Electrons move, ions shift position, interfaces change over time to adapt, perform computation and store information within the same physical substance, all in real time. This continuous motion expands the effective dimensionality of neural computation by converting static structural degrees of freedom into time-varying computational states.

We have shown that the spatiotemporal resolution of signals sent to the brain depends on the eye's sampling patterns: a combination of saccades and brief fixations, photoreceptor density, and spatiotemporal and morphodynamic interactions within the retinal network. Through stochastic refractory quantal sampling of photons and transmitter molecules, together with delay-minimising processes such as high-frequency synaptic jumping, the visual system can rapidly adapt its signalling capacity across diverse contexts. These mechanisms generate bursty, highly reliable, high-acuity spatiotemporal representations of environmental objects that support visual invariance. More broadly, they may supply a shared internal representational substrate - a common neural "vocabulary" - for efficient communication within and across brain circuits.

Beyond these immediate benefits, what additional evolutionary advantages do multiscale, motion-based neural computations confer?

From a modelling perspective, the energy efficiency of quantal and compartmentalised biochemical computation is striking. By contrast, computing with action potentials is energetically expensive [248]. Energetic estimates highlight a large gap between electrical and biochemical information processing: an action potential costs on the order of ~7×10^8 ATP, whereas synaptic and biochemical signalling can transmit information at far lower ATP cost, for example ~10^4 ATP per bit at a chemical synapse versus ~10^6–10^7 ATP per bit for graded or spike-based codes [164]. This disparity motivates the design principle that evolution 'computes with chemistry' wherever possible. Thus, depending on the operation and level of abstraction, transformations that would require spike-based electrical signalling can incur 3-6 orders of magnitude lower energetic expenditure when implemented biochemically [249]. This cost-benefit disparity suggests that evolution favours computational strategies that offload a substantial fraction of processing from action potentials to molecular, photomechanical, and enzymatic interactions. In classical neuroscience, neurons have been treated as the primary computational units, with synapses viewed largely as passive interconnects.

We propose the inverse perspective. Much of the brain's computation occurs in the biochemical domain rather than the electrical one. Operations analogous to multiplication and division emerge naturally from precisely timed, logarithmically varying numbers of quantal samples, orchestrated by

enzymatic cascades and amplified by physical motion, including the participating molecules' charge–polarity interactions, and molecular motor activity. Concrete examples include the phototransduction cascade within individual microvilli, compartmentalised calcium- and enzyme-mediated reactions, and the densely interconnected synaptic microcircuits distributed throughout the brain.

From this viewpoint, neural information processing can be described at two complementary levels of abstraction. NeuroCentric models preserve the traditional neuron-level framework, maintaining continuity with established theories of spiking, coding, and networks. SynaptoCentric models, by contrast, treat ensembles of synapses and their biochemical microcircuits as the primary computational units. In these models, information is transmitted through stochastic, refractory, quantal sampling, while neurons function primarily as the wiring that couples computational micro-networks. This shift from predominantly electrical to biochemical computation offers a more energy-efficient and biologically grounded account of neural processing. In morphodynamic multiscale models, NeuroCentric components provide conceptual continuity, whereas SynaptoCentric components open a path toward fundamentally new understandings of how brains compute.

2.6. Single-Neuron Encoding Is Precise, Yet Every Neuron Responds Uniquely

Neural computations are often viewed as "noisy", leading to the idea that the brain uses probabilistic parallel processing to extract meaning from the variable signalling of individual neurons. The "Bayesian brain" hypothesis proposes that the brain operates like a probability machine, using Bayesian inference to process information [250–252]. It assumes the brain makes continuous predictions about the world and updates them based on sensory input, weighing prior knowledge against new evidence. The difference between prediction and input is a prediction error, which the brain uses to refine future predictions [253]. In this view, the brain maintains a generative model of the world: a network of probabilistic beliefs that allows it to anticipate incoming sensory data. One proposed assumption is that the noisy spiking activity of neurons constitutes a form of sampling from the relevant probability distribution. The instantaneous pattern of spikes is treated as a sample, while activity averaged over time or across populations estimates the underlying distribution. Perception is thus viewed as inference about the causes of sensory data, and actions as attempts to fulfil predictions or reduce prediction errors.

However, given what we now know, that each sensory neuron continuously integrates vast numbers of stochastic quantal refractory samples to produce near noise-free responses [3,24,26,27], there is little reason to assume that cortical neurons perform their computations with greater "internal" noise or less precision than sensory neurons engaged in edge computing. Throughout an animal, neurons are connected by vast numbers of synapses, share the same molecular constituents, and each contributes to coordinated bodily functions, the integration of thoughts and actions, and the planning of the next step. The system would not be reliable if some parts had somehow evolved to operate far less efficiently than others. When we see the benefits of multi-scale morphodynamic motion at the edge in accelerating and enhancing encoding and signalling, it is only logical to expect that similar mechanisms are also at play more centrally.

Figure 13 illustrates that voltage responses of both graded-potential and spiking neurons are highly repeatable and therefore low-noise. Whether at the sensory periphery or deeper in the brain, morphodynamic integration of variable quantal synaptic inputs produces reliable responses, including highly precise action-potential waveforms, that faithfully and rapidly encode changes in the synaptic input-conductance state. This precision holds irrespective of whether the transmitted information is predominantly syntactic (Shannon) or part of a semantic code.

This realisation emphasises that neurons throughout the nervous system - whether photoreceptors [24,27], visual interneurons [10,27,49,80], cerebellar granule cells [102,254,255], hippocampal mossy fibres [256], or cortical neurons [257–259] - have evolved to work efficiently with the laws of physics, not against them. Neural sampling and processing exploit quantal stochasticity and ultrastructural motion to enhance and accelerate encoding, rather than expending additional

effort to minimise or suppress these sources of variability as noise. Consequently, models seeking to describe these systems must operate within the same physical constraints, adapting across scales to incorporate biophysical and physiological realism. After all, neurons within an organism share the same genetic code that governs and adapts their specific structure-function relationships to changing conditions, while relying on the same molecular building blocks - proteins and lipids that form ubiquitous ion channels, transporters, neurotransmitters, and intra- and extracellular scaffolding - throughout the nervous system.

Accordingly, increasing evidence shows that an action-potential waveform is, in terms of precision, no different from a non-spiking graded waveform [257,258] (**Figure 13**). Both are sculpted by morphodynamic stochastic synaptic quantal sampling, arising from the ~10,000-30,000 synaptic inputs converging onto a typical cortical neuron [260–263], and by a diverse complement of voltage-sensitive ion channels that transiently accentuate phasic input changes, forming part of an efficient refractory code that informs neighbouring neurons about ongoing events. Theoretically, the resulting precision can be analogous to that achieved in insect photoreceptors through morphodynamic quantal stochastic refractory photon sampling in ~30,000-90,000 microvilli (cf. **Figures 5-6**).

Across species and nervous systems, individual neurons, with each defined by its unique structure-function architecture, generate highly precise responses to meaningful stimuli. Neighbouring neurons are similarly low-noise, yet their response waveforms differ from cell to cell. Such structured variability is not noise but complementary information. When two neurons synapse onto a third and convey slightly different versions of the same stimulus, the receiving neuron can combine these signals to form more accurate and robust estimates of specific stimulus features [264] - for example, how the same visual object appears at two nearby points in space.
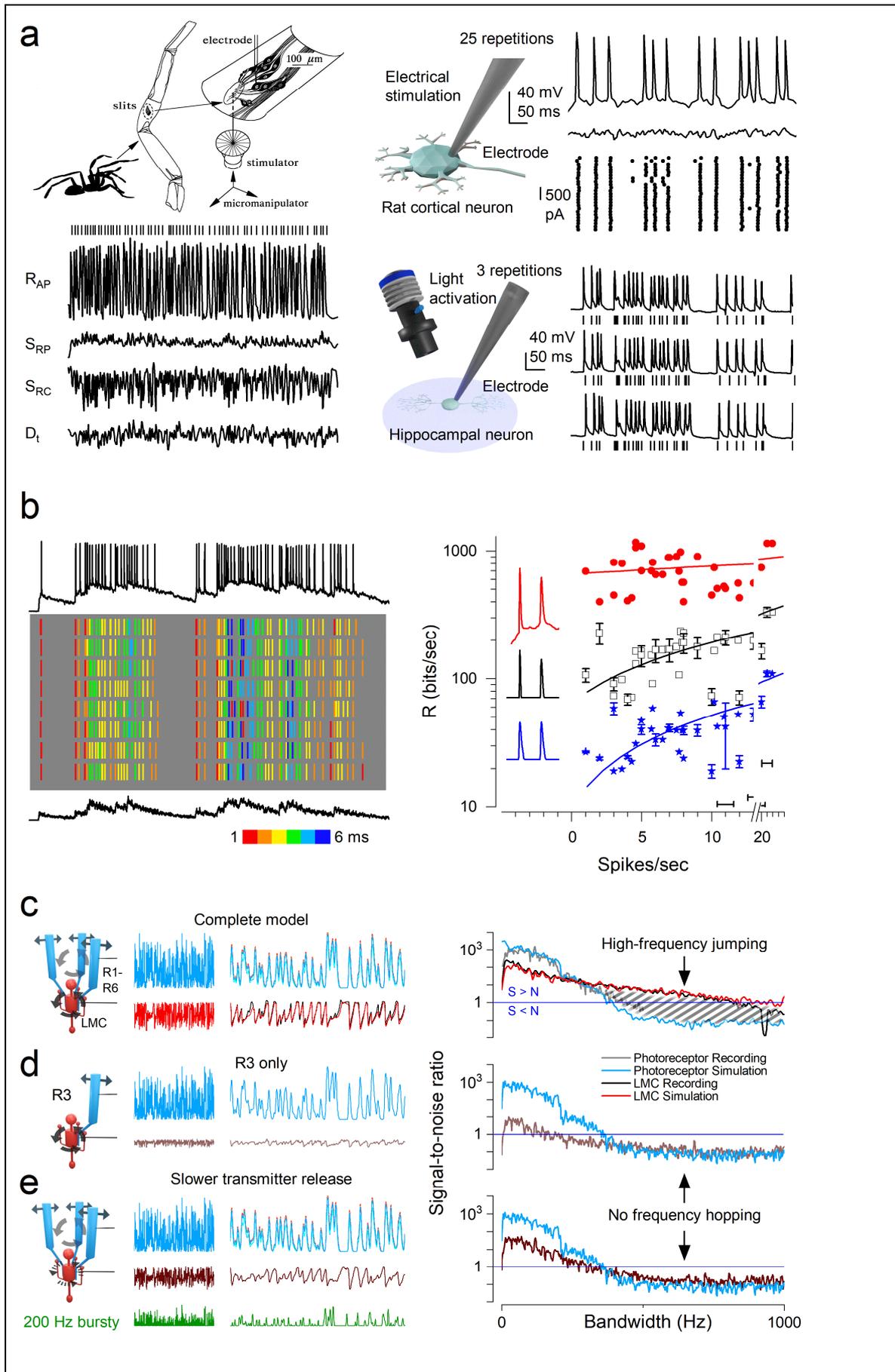
Figure 13. The responses of both spiking and graded-potential neurons are precise, with encoding generating accurate waveforms at sub-millisecond resolution, yet each neuron responds uniquely. (**a**) Intracellularly

recorded neuronal responses to fast dynamic stimulation are highly repeatable both in sensory and cortical neurons. Left: action potentials (R_{AP}), receptor potential (S_{RP}) and receptor current (S_{RC}) of a wandering spider (*Cupienus salei*) slit sensilla mechanoreceptor to the same white-noise modulated cuticular displacement stimulus (D_s) [265]. Receptor current (under voltage-clamp) and receptor potential (under current clamp) were recorded after blocking action potentials with tetrodotoxin. Right: action potential of cortical neurons evoked by fluctuating current injection (above) [266] or optogenetic light pulses [267] (below). Intracellular recordings across repeated presentations of the same stimulus show highly reproducible stimulus-dependent action-potential waveforms and timing (interspike intervals) at sub-millisecond precision. Right, above: recordings from a regular-firing layer-5 pyramidal neuron. Fluctuating Gaussian white-noise stimulus parameters: μ_s = 150 pA, σ_s = 100 pA, τ_s = 3 ms. Right, below: a single hippocampal neuron stimulated optogenetically with repeated pulse trains exhibits strikingly similar spike timing and waveform structure across trials, demonstrating low intrinsic noise. (**b**) Voltage response (top trace; 40 mV) of a layer-5 neuron to a bursting pattern of AMPA conductance events (bottom trace; 5 nS, 1 s) at 34 °C [257]. Between these traces are the corresponding colour-coded spike-time widths across eight trials. Right: information-transfer rates of pyramidal neurons (n = 21) for different conductance patterns (stationary and nonstationary) plotted against mean firing rate. Information was calculated from the full-voltage responses (red circles), the action-potential waveforms (white squares), and stereotyped spikes (blue stars), sampled at 2 kHz. Inset: short segment of all three signals, each containing two spikes. Information rate R increases linearly with firing rate f in each case (full voltage: r = 10.4 × f + 660.6; spike waveforms: r = 12.9 × f + 64.7; stereotyped spikes: r = 4.2 × f + 9.8). (**c**) Complete photoreceptor–LMC model [27] reproduces high-frequency jumping (see **Figure 4a**, **b**). Left: simulated R1–R6 photoreceptor and postsynaptic LMC responses (blue and red) under naturalistic input show high-frequency, precise waveform fluctuations. Right: corresponding signal-to-noise ratio (SNR) spectra for recordings (solid) and simulations (dashed) reveal high-frequency jumping (S greater than N), emerging from coordinated synaptic integration in the full circuit. (**d**) R3-only model lacks high-frequency enhancement. Removing synaptic convergence (single-input model) lowers gain and prevents synaptic clipping (cf. **Figure 4e**), greatly reducing the SNR of ultrafast fluctuations in LMC responses. Corresponding SNR spectra show no high-frequency jumping, indicating that convergence and population sampling are essential for this emergent precision. (**e**) Slower transmitter (histamine) release abolishes high-frequency jumping. Artificially slowing synaptic transmission in the full model dampens rapid LMC modulations (brown trace) and eliminates high-frequency enhancement in the SNR spectrum. A 200 Hz bursty input train (green) is included for comparison. Together, these panels demonstrate that precise yet unique neural responses arise from rapid quantal sampling, convergent synaptic input, and morphodynamic circuit mechanisms.

This principle is clearly demonstrated by experiments and simulations in the morphodynamic neural superposition system of the compound eye (**Figure 13c-e**). Each R1-R6 photoreceptor feeding a single LMC has a signal-to-noise ratio of several thousand and carries ~2,000-2,500 bits s⁻¹ under bursty, saccade-like input. Because six partly overlapping photoreceptor channels converge onto the same LMC, and because synaptic high-frequency jumping reduces delays and enhances timing precision during transmission, the resulting LMC information rate can exceed ~4,000 bits s⁻¹. The slight differences across photoreceptor inputs therefore enhance, rather than degrade, downstream encoding accuracy.

Conclusion

Despite major advances in understanding the brain's chemical and electrical processes, neuroscience still often assumes that neurons act as static, band-limited filters degraded by additive noise. We propose instead that neural signalling is a morphodynamic, adaptive process in which variability is integral rather than detrimental, driven by active sensing within closed sensory–motor loops to accelerate and enhance encoding. The brain's functional connectome is organised genetically to map the physical regularities of the world. By using continuous stochastic changes in quantal sampling, embodied in unitary response waveforms, latencies, refractoriness, and ultrastructural dynamics, neurons can integrate reliable, virtually noise-free, and phasic representations of the world

with minimal delay. These representations are inherently anti-aliased, auto-scaled, and capable of hyperacute spatiotemporal precision, particularly during active behaviours.

Our framework, grounded in neuronal and synaptic models incorporating adaptive quantal sampling, formalises the distributed and compartmentalised computation observed in real neurons. Supported by simulations and emerging experimental evidence, it redefines response variability ("noise") as a functional resource for robust coding and identifies morphodynamics as a key mechanism linking structure and function. Beyond explaining neural precision and adaptability, this perspective offers testable experimental predictions, inspires bio-inspired AI, and challenges conventional models of sequential information processing in the brain.

References

1. Shannon CE. A mathematical theory of communication. Bell Syst Technic J. 1948;27:379–423, 623–56.
2. Borst A, Theunissen FE. Information theory and neural coding. Nat Neurosci. 1999;2:947-57.
3. Juusola M, Takalo J, Kemppainen J, Razban Haghighi K, Scales B, McManus J, et al. Theory of morphodynamic information processing: linking sensing to behaviour. Vision Res. 2025;227.
4. Perez-Escudero A, Rivera-Alba M, de Polavieja GG. Structure of deviations from optimality in biological systems. Proc Natl Acad Sci U S A. 2009;106:20544-9.
5. Rivera-Alba M, Vitaladevuni SN, Mischenko Y, Lu ZY, Takemura SY, Scheffer L, et al. Wiring economy and volume exclusion determine neuronal placement in the *Drosophila* brain. Curr Biol. 2011;21:2000-5.
6. de Polavieja GG. Errors drive the evolution of biological signalling to costly codes. J Theor Biol. 2002;214:657-64.
7. Song Z, Juusola M. Refractory sampling links efficiency and costs of sensory encoding to stimulus statistics. J Neurosci. 2014;34:7216-37.
8. Barlow HB. Possible principles underlying the transformations of sensory messages. In: Rosenblith W, editor. Sensory Communication: M.I.T. Press; 1961. p. 217-34.
9. Darwin C. On the origin of species by means of natural selection, or the preservation of favoured races in the struggle for life. London: John Murray; 1859.
10. Juusola M, French AS, Uusitalo RO, Weckstrom M. Information processing by graded-potential transmission through tonically active synapses. Trends Neurosci. 1996;19:292-7.
11. Reshetniak S, Rizzoli SO. The vesicle cluster as a major organizer of synaptic composition in the short-term and long-term. Curr Opin Cell Biol. 2021;71:63-8.
12. Reshetniak S, Ussling JE, Perego E, Rammner B, Schikorski T, Fornasiero EF, et al. A comparative analysis of the mobility of 45 proteins in the synaptic bouton. Embo J. 2020;39.
13. Rusakov DA, Savtchenko LP, Zheng KY, Henley JM. Shaping the synaptic signal: molecular mobility inside and outside the cleft. Trends Neurosci. 2011;34:359-69.
14. Watanabe S, Rost BR, Camacho-Perez M, Davis MW, Sohl-Kielczynski B, Rosenmund C, et al. Ultrafast endocytosis at mouse hippocampal synapses. Nature. 2013;504:242-7.
15. El Hady A, Machta BB. Mechanical surface waves accompany action potential propagation. Nat Commun. 2015;6.
16. Kasai H, Ucar H. Forceful synapses reveal mechanical interactions in the brain. Nature. 2021.
17. Korkotian E, Segal M. Spike-associated fast contraction of dendritic spines in cultured hippocampal neurons. Neuron. 2001;30:751-8.
18. Majewska A, Sur M. Motility of dendritic spines in visual cortex in vivo: changes during the critical period and effects of visual deprivation. Proc Natl Acad Sci U S A. 2003;100:16024-9.

19. Ucar H, Watanabe S, Noguchi J, Morimoto Y, Iino Y, Yagishita S, et al. Mechanical actions of dendritic-spine enlargement on presynaptic exocytosis. Nature. 2021;600:686-9.

20. Benoit CM, Ganea DA, Paricio-Montesinos R, Esser J, Thome C, Janssen JM, et al. Axon initial segment dynamics during associative fear learning. Nat Neurosci. 2025.

21. Yu WQ, Swanstrom R, Sigulinsky CL, Ahlquist RM, Knecht S, Jones BW, et al. Distinctive synaptic structural motifs link excitatory retinal interneurons to diverse postsynaptic partner types. Cell Rep. 2023;42:112006.

22. Kennedy HJ, Crawford AC, Fettiplace R. Force generation by mammalian hair bundles supports a role in cochlear amplification. Nature. 2005;433:880-3.

23. Hardie RC, Franze K. Photomechanical responses in *Drosophila* photoreceptors. Science. 2012;338:260-163.

24. Juusola M, Dau A, Song Z, Solanki N, Rien D, Jaciuch D, et al. Microsaccadic sampling of moving image information provides *Drosophila* hyperacute vision. Elife. 2017;6.

25. Kemppainen J, Mansour N, Takalo J, Juusola M. High-speed imaging of light-induced photoreceptor microsaccades in compound eyes. Commun Biol. 2022;5:203.

26. Kemppainen J, Scales B, Razban Haghighi K, Takalo J, Mansour N, McManus J, et al. Binocular mirror-symmetric microsaccadic sampling enables *Drosophila* hyperacute 3D vision. Proc Natl Acad Sci U S A. 2022;119:e2109717119.

27. Mansour N, Takalo J, Kemppainen J, Bridges AD, MaBouDi H, Bohra AA, et al. Synaptic high-frequency jumping synchronises vision to high-speed behaviour. BioRxiv. 2025.

28. Bocchero U, Falleroni F, Mortal S, Li Y, Cojoc D, Lamb T, et al. Mechanosensitivity is an essential component of phototransduction in vertebrate rods. PLoS Biol. 2020;18:e3000750.

29. Pandiyan VP, Maloney-Bertelli A, Kuchenbecker JA, Boyle KC, Ling T, Chen ZC, et al. The optoretinogram reveals the primary steps of phototransduction in the living human eye. Sci Adv. 2020;6.

30. Joy MSH, Nall DL, Emon B, Lee KY, Barishman A, Ahmed M, et al. Synapses without tension fail to fire in an in vitro network of hippocampal neurons. Proc Natl Acad Sci U S A. 2023;120:e2311995120.

31. Juusola M, Song ZY. How a fly photoreceptor samples light information in time. J Physiol Lond. 2017;595:5427-37.

32. Song Z, Postma M, Billings SA, Coca D, Hardie RC, Juusola M. Stochastic, adaptive sampling of information by microvilli in fly photoreceptors. Curr Biol. 2012;22:1371-80.

33. Hubel DH, Wiesel TN. Visual area of the lateral suprasylvian gyrus (Clare-Bishop area) of the cat. J Physiol. 1969;202:251-60.

34. Hubel DH, Wiesel TN. Stereoscopic vision in macaque monkey. Cells sensitive to binocular depth in area 18 of the macaque monkey cortex. Nature. 1970;225:41-2.

35. Mountcastle VB. Modality and topographic properties of single neurons of cat's somatic sensory cortex. J Neurophysiol. 1957;20:408-34.

36. Mountcastle VB. The columnar organization of the neocortex. Brain. 1997;120 (Pt 4):701-22.

37. Békésy Gv. Über die Schwingungen der Basilarmembran beim Hören. Physikalische Zeitschrift. 1928;29:793-810.

38. Galambos R, Davis H. Electrophysiological evidence of tonotopic organization in the auditory cortex of the cat. Journal of Neurophysiology. 1948;11:431-9.

39. Tunturi AR. Physiological determination of the tonotopic organization of the auditory cortex in the dog. American Journal of Physiology. 1950;162:562–8.

40. Olson CR, Graybiel AM. Sensory maps in the claustrum of the cat. Nature. 1980;288:479-81.

41. Lee KS, Loutit AJ, de Thomas Wagner D, Sanders M, Huber D. Emergence of a brainstem somatosensory tonotopic map for substrate vibration. Nat Neurosci. 2025;28:97-104.

42. Li M, Liu F, Juusola M, Tang S. Perceptual color map in macaque visual area V4. J Neurosci. 2014;34:202-17.

43. Merzenich MM, Knight PL, Roth GL. Cochleotopic organization of primary auditory cortex in the cat. Brain Res. 1973;63:343-6.

44. Merzenich MM, Knight PL, Roth GL. Representation of cochlea within primary auditory cortex in the cat. J Neurophysiol. 1975;38:231-49.

45. Kohonen T. Self-organizing neural projections. Neural Netw. 2006;19:723-33.

46. Kohonen T, Hari R. Where the abstract feature maps of the brain might come from. Trends Neurosci. 1999;22:135-9.

47. Fernandes AR, Martins JP, Gomes ER, Mendes CS, Teodoro RO. *Drosophila* motor neuron boutons remodel through membrane blebbing coupled with muscle contraction. Nat Commun. 2023;14.

48. Griswold JM, Bonilla-Quintana M, Pepper Rea. Membrane mechanics dictate axonal pearls-on-a-string morphology and function. Nat Neurosci. 2025;28:49-61.

49. Zheng L, de Polavieja GG, Wolfram V, Asyali MH, Hardie RC, Juusola M. Feedback network controls photoreceptor output at the layer of first visual synapses in *Drosophila*. J Gen Physiol. 2006;127:495-510.

50. Wong F, Knight BW. Adapting-bump model for eccentric cells of Limulus. J Gen Physiol. 1980;76:539-57.

51. Wong F, Knight BW, Dodge FA. Dispersion of latencies in photoreceptors of Limulus and the adapting-bump model. J Gen Physiol. 1980;76:517-37.

52. Baylor DA, Lamb TD, Yau KW. Responses of retinal rods to single photons. J Physiol. 1979;288:613-34.

53. Faisal AA, Selen LPJ, Wolpert DM. Noise in the nervous system. Nat Rev Neurosci. 2008;9:292-303.

54. Laughlin SB. The role of sensory adaptation in the retina. J Exp Biol. 1989;146:39-62.

55. Laughlin SB, Howard J, Blakeslee B. Synaptic limitations to contrast coding in the retina of the blowfly Calliphora. Proc R Soc Lond B Biol Sci. 1987;231:437-67.

56. Laughlin SB, Lillywhite PG. Intrinsic noise in locust photoreceptors. J Physiol. 1982;332:25-45.

57. Lillywhite PG, Laughlin SB. Transducer noise in a photoreceptor. Nature. 1979;277:569-72.

58. Amari S, Takeuchi A. Mathematical theory on formation of category detecting nerve cells. Biol Cybern. 1978;29:127-36.

59. Takeuchi A, Amari S. Formation of topographic maps and columnar microstructures in nerve fields. Biol Cybern. 1979;35:63-72.

60. Sjoberg RL. Brain stimulation and elicited memories. Acta Neurochir (Wien). 2023;165:2737-45.

61. Suthana N, Fried I. Percepts to recollections: insights from single neuron recordings in the human brain. Trends Cogn Sci. 2012;16:427-36.

62. Panzeri S, Senatore R, Montemurro MA, Petersen RS. Correcting for the sampling bias problem in spike train information measures. Journal of Neurophysiology. 2007;98:1064-72.

63. Zheng JY, Meister M. The unbearable slowness of being: Why do we live at 10 bits/s? Neuron. 2025;113:192-204.

64. Rieke F, Bodnar DA, Bialek W. Naturalistic stimuli increase the rate and efficiency of information transmission by primary auditory afferents. Proc Biol Sci. 1995;262:259-65.

65. Lazar AA, Liu TK, Yeh CH. The functional logic of odor information processing in the antennal lobe. Plos Comput Biol. 2023;19.

66. Atick JJ, Redlich AN. Towards a theory of early visual processing. Neural Computation. 1990;2:308-20.

67. van Hateren JH. A theory of maximizing sensory information. Biol Cybern. 1992;68:23-9.

68. Hubel DH, Wiesel TN. Uniformity of monkey striate cortex: a parallel relationship between field size, scatter, and magnification factor. J Comp Neurol. 1974;158:295-305.

69. Hubel DH, Wiesel TN. Sequence regularity and geometry of orientation columns in the monkey striate cortex. J Comp Neurol. 1974;158:267-93.

70. Ahissar E, Arieli A. Figuring space by time. Neuron. 2001;32:185-201.

71. Casile A, Victor JD, Rucci M. Contrast sensitivity reveals an oculomotor strategy for temporally encoding space. Elife. 2019;8.

72. Intoy J, Li YH, Bowers NR, Victor JD, Poletti M, Rucci M. Consequences of eye movements for spatial selectivity. Current Biology. 2024;34.

73. Kuang X, Poletti M, Victor JD, Rucci M. Temporal encoding of spatial information during active visual fixation. Curr Biol. 2012;22:510-4.

74. Rucci M, Ahissar E, Burr DC, Kagan I, Poletti M, Victor JD. The visual system does not operate like a camera. J Vis. 2025;25:2.

75. Rucci M, Victor JD. The unsteady eye: an information-processing stage, not a bug. Trends in Neurosciences. 2015;38:195-206.

76. Rucci M, Iovin R, Poletti M, Santini F. Miniature eye movements enhance fine spatial detail. Nature. 2007;447:851-4.

77. Juusola M, Uusitalo RO, Weckstrom M. Transfer of graded potentials at the photoreceptor-interneuron synapse. J Gen Physiol. 1995;105:117-48.

78. Meinertzhagen IA, O'Neil SD. Synaptic organization of columnar elements in the lamina of the wild type in *Drosophila melanogaster*. J Comp Neurol. 1991;305:232-63.

79. Nikolaev A, Zheng L, Wardill TJ, O'Kane CJ, de Polavieja GG, Juusola M. Network adaptation improves temporal representation of naturalistic stimuli in *Drosophila* eye: II mechanisms. PLoS One. 2009;4:e4306.

80. Zheng L, Nikolaev A, Wardill TJ, O'Kane CJ, de Polavieja GG, Juusola M. Network adaptation improves temporal representation of naturalistic stimuli in *Drosophila* eye: I dynamics. PLoS One. 2009;4:e4307.

81. Buschbeck EK, Hoy RR. Visual system of the stalk-eyed fly, Cyrtodiopsis quinqueguttata (Diopsidae, Diptera): an anatomical investigation of unusual eyes. J Neurobiol. 1998;37:449-68.

82. Teich MC, Prucnal PR, Vannucci G, Breton ME, Mcgill WJ. Multiplication Noise in the Human Visual-System at Threshold .1. Quantum Fluctuations and Minimum Detectable Energy. J Opt Soc Am. 1982;72:419-31.

83. Warrant EJ. The remarkable visual capacities of nocturnal insects: vision at the limits with small eyes and tiny brains. Philos T R Soc B. 2017;372.

84. Tang S, Juusola M. Intrinsic activity in the fly brain gates visual information during behavioral choices. PLoS One. 2010;5:e14455.

85. Franceschini N. Combined optical neuroanatomical, electrophysiological and behavioural studies on signal processing in the fly compound eye. In: Taddei-Ferretti C, editor. Biocybernetics of Vision: Integrative Mechanisms and Cognitive Processes. Singapore: World Scientific; 1998. p. 341-61.

86. Howard J, Blakeslee B, Laughlin SB. The intracellular pupil mechanism and photoreceptor signal: noise ratios in the fly *Lucilia cuprina*. Proc R Soc Lond B Biol Sci. 1987;231:415-35.

87. Enroth-Cugell C, Robson JG. The contrast sensitivity of retinal ganglion cells of the cat. J Physiol. 1966;187:517-52.

88. Juusola M. Linear and nonlinear contrast coding in light-adapted blowfly photoreceptors. J Comp Physiol A. 1993;172:511-21.

89. Hartline HK, Wagner HG, Ratliff F. Inhibition in the Eye of Limulus. Journal of General Physiology. 1956;39:651-73.

90. Hartline HK, Graham CH. Nerve impulses from single receptors in the eye of limulus. P Soc Exp Biol Med. 1932;29:0613-5.

91. Livingstone MS, Hubel DH. Spatial relationship and extrafoveal vision. Nature. 1985;315:285.

92. Zhang SH, Zhao XN, Jiang DQ, Tang SM, Yu C. Ocular dominance-dependent binocular combination of monocular neuronal responses in macaque V1. Elife. 2024;13.

93. Ju NS, Guan SC, Tao L, Tang SM, Yu C. Orientation Tuning and End-stopping in Macaque V1 Studied with Two-photon Calcium Imaging. Cereb Cortex. 2021;31:2085-97.

94. Gonzalez-Bellido PT, Wardill TJ, Juusola M. Compound eyes and retinal information processing in miniature dipteran species match their specific ecological demands. Proc Natl Acad Sci U S A. 2011;108:4224-9.

95. van Hateren JH. Real and optimal neural images in early vision. Nature. 1992;360:68-70.

96. Yau KW, Lamb TD, Baylor DA. Light-induced fluctuations in membrane current of single toad rod outer segments. Nature. 1977;269:78-80.

97. Normann RA, Werblin FS. Control of retinal sensitivity. I. Light and dark adaptation of vertebrate rods and cones. J Gen Physiol. 1974;63:37-61.

98. Laughlin SB, Hardie RC. Common Strategies for Light Adaptation in the Peripheral Visual Systems of Fly and Dragonfly. J Comp Physiol. 1978;128:319-40.

99. Baylor DA, Hodgkin AL, Lamb TD. Reconstruction of the electrical responses of turtle cones to flashes and steps of light. J Physiol. 1974;242:759-91.

100. Baylor DA, Hodgkin AL, Lamb TD. The electrical response of turtle cones to flashes and steps of light. J Physiol. 1974;242:685-727.

101. Juusola M, Hardie RC. Light adaptation in *Drosophila* photoreceptors: II. Rising temperature increases the bandwidth of reliable signaling J Gen Physiol. 2001;117:27–42.

102. Saviane C, Silver RA. Fast vesicle reloading and a large pool sustain high bandwidth transmission at a central synapse. Nature. 2006;439:983-7.

103. Laughlin SB. A simple coding procedure enhances a neuron's information capacity. Zeitschrift für Naturforschung C. 1981;36:910-2.

104. van Hateren JH. Processing of natural time series of intensities by the visual system of the blowfly. Vision Res. 1997;37:3407-16.

105. van Hateren JH. Theoretical predictions of spatiotemporal receptive fields of fly LMCs, and experimental validation. J Comp Physiol A. 1992;171:157-70.

106. Brenner N, Bialek W, de Ruyter van Steveninck R. Adaptive rescaling maximizes information transmission. Neuron. 2000;26:695-702.

107. Attneave F. Some informational aspects of visual perception. Psychol Rev. 1954;61:183-93.

108. Juusola M, Weckstrom M, Uusitalo RO, Korenberg MJ, French AS. Nonlinear models of the first synapse in the light-adapted fly retina. J Neurophysiol. 1995;74:2538-47.

109. Juusola M, Kouvalainen E, Jarvilehto M, Weckstrom M. Contrast gain, signal-to-noise ratio, and linearity in light-adapted blowfly photoreceptors. J Gen Physiol. 1994;104:593-621.

110. van Hateren JH, Schilstra C. Blowfly flight and optic flow II. Head movements during flight. J Exp Biol. 1999;202:1491-500.

111. de Ruyter van Steveninck RR, Laughlin SB. The rate of information transfer at graded-potential synapses. Nature. 1996:642-5.

112. Juusola M, Hardie RC. Light Adaptation in *Drosophila* Photoreceptors: I. Response Dynamics and Signaling Efficiency at 25 °C. J Gen Physiol. 2001;117:3-25.

113. van Hateren JH, Snippe HP. Information theoretical evaluation of parametric models of gain control in blowfly photoreceptor cells. Vision Res. 2001;41:1851-65.

114. van Hateren JH, Snippe HP. Phototransduction in primate cones and blowfly photoreceptors: different mechanisms, different algorithms, similar response. J Comp Physiol A Neuroethol Sens Neural Behav Physiol. 2006;192:187-97.

115. Juusola M, de Polavieja GG. The rate of information transfer of naturalistic stimulation by graded potentials. J Gen Physiol. 2003;122:191-206.

116. Blaj G, van Hateren JH. Saccadic head and thorax movements in freely walking blowflies. J Comp Physiol A Neuroethol Sens Neural Behav Physiol. 2004;190:861-8.

117. Lindemann JP, Kern R, Michaelis C, Meyer P, van Hateren JH, Egelhaaf M. FliMax, a novel stimulus device for panoramic and highspeed presentation of behaviourally generated optic flow. Vision Res. 2003;43:779-91.

118. Schilstra C, Van Hateren JH. Blowfly flight and optic flow I. Thorax kinematics and flight dynamics. J Exp Biol. 1999;202:1481-90.

119. van Hateren JH, van der Schaaf A. Independent component filters of natural images compared with simple cells in primary visual cortex. Proc Roy Soc Lond B. 1998;265:359-66.

120. Atick JJ. Could information theory provide an ecological theory of sensory processing? Network. 2011;22:4-44.

121. Dan Y, Atick JJ, Reid RC. Efficient coding of natural scenes in the lateral geniculate nucleus: experimental test of a computational theory. J Neurosci. 1996;16:3351-62.

122. van Hateren JH, Ruttiger L, Sun H, Lee BB. Processing of natural temporal stimuli by macaque retinal ganglion cells. J Neurosci. 2002;22:9945-60.

123. Schilstra C, van Hateren JH. Using miniature sensor coils for simultaneous measurement of orientation and position of small, fast-moving animals. J Neurosci Methods. 1998;83:125-31.

124. Fenk LM, Avritzer SC, Weisman JL, Nair A, Randt LD, Mohren TL, et al. Muscles that move the retina augment compound eye vision in *Drosophila*. Nature. 2022;612:116-22.

125. Franceschini N, Chagneux R, Kirschfeld K. Gaze control in flies by co-ordinated action of eye muscles. In: Elsner N, Menzel R, editors. Gottingen Neurobiology Report1995. p. 401.

126. MaBouDi H, Roper M, Guiraud M-G, Chittka L, Marshall JA. A neuromorphic model of active vision shows how spatiotemporal encoding in lobula neurons can aid pattern recognition in bees. eLife. 2023;14.

127. Juusola M, Song Z, Hardie RC. Phototransduction Biophysics. In: Jaeger D, Jung R, editors. Encyclopedia of Computational Neuroscience. New York, NY: Springer; 2022. p. 2758-76.

128. Song Z, Zhou Y, Feng J, Juusola M. Multiscale 'whole-cell' models to study neural information processing - New insights from fly photoreceptor studies. J Neurosci Methods. 2021;357:109156.

129. Hardie RC, Juusola M. Phototransduction in *Drosophila*. Curr Opin Neurobiol. 2015;34:37-45.

130. Faivre O, Juusola M. Visual coding in locust photoreceptors. Plos One. 2008;3.

131. Bastos AM, Usrey WM, Adams RA, Mangun GR, Fries P, Friston KJ. Canonical Microcircuits for Predictive Coding. Neuron. 2012;76:695-711.

132. Rao RPN, Ballard DH. Predictive coding in the visual cortex: a functional interpretation of some extra-classical receptive-field effects. Nat Neurosci. 1999;2:79-87.

133. Friston KJ. A theory of cortical responses. Philos T R Soc B. 2005;360:815-36.

134. Sommer MA, Wurtz RH. Brain circuits for the internal monitoring of movements. Annual Review of Neuroscience. 2008;31:317-38.

135. Sperry RW. Neural Basis of the Spontaneous Optokinetic Response Produced by Visual Inversion. J Comp Physiol Psych. 1950;43:482-9.

136. von Holst E, Mittelstaedt H. Das Reafferenzprinzip - (Wechselwirkungen Zwischen Zentralnervensystem Und Peripherie). Naturwissenschaften. 1950;37:464-76.

137. Skingsley DR, Laughlin SB, Hardie RC. Properties of Histamine-Activated Chloride Channels in the Large Monopolar Cells of the Dipteran Compound Eye - a Comparative-Study. J Comp Physiol A. 1995;176:611-23.

138. Hardie RC. A Histamine-Activated Chloride Channel Involved in Neurotransmission at a Photoreceptor Synapse. Nature. 1989;339:704-6.

139. Hardie RC. Effects of Antagonists on Putative Histamine-Receptors in the 1st Visual Neuropil of the Housefly (Musca-Domestica). J Exp Biol. 1988;138:221-41.

140. Nassel DR, Holmqvist MH, Hardie RC, Hakanson R, Sundler F. Histamine-Like Immunoreactivity in Photoreceptors of the Compound Eyes and Ocelli of the Flies Calliphora-Erythrocephala and Musca-Domestica. Cell Tissue Res. 1988;253:639-46.

141. Hardie RC. Is Histamine a Neurotransmitter in Insect Photoreceptors. J Comp Physiol A. 1987;161:201-13.

142. Dau A, Friederich U, Dongre S, Li X, Bollepalli MK, Hardie RC, et al. Evidence for Dynamic Network Regulation of Drosophila Photoreceptor Function from Mutants Lacking the Neurotransmitter Histamine. Front Neural Circuits. 2016;10:19.

143. Yau KW, Hardie RC. Phototransduction motifs and variations. Cell. 2009;139:246-64.

144. Fain GL, Hardie R, Laughlin SB. Phototransduction and the evolution of photoreceptors. Curr Biol. 2010;20:R114-24.

145. Wardill TJ, List O, Li X, Dongre S, McCulloch M, Ting CY, et al. Multiple spectral inputs improve motion discrimination in the *Drosophila* visual system. Science. 2012;336:925-31.

146. Poulet JF, Hedwig B. New insights into corollary discharges mediated by identified neural pathways. Trends Neurosci. 2007;30:14-21.

147. Hochstrate P, Hamdorf K. Microvillar components of light adaptation in blowflies. J Gen Physiol. 1990;95:891-910.

148. Pumir A, Graves J, Ranganathan R, Shraiman BI. Systems analysis of the single photon response in invertebrate photoreceptors. Proc Natl Acad Sci U S A. 2008;105:10354-9.

149. Liu CH, Satoh AK, Postma M, Huang J, Ready DF, Hardie RC. Ca^{2+}-dependent metarhodopsin inactivation mediated by calmodulin and NINAC myosin III. Neuron. 2008;59:778-89.

150. Mishra P, Socolich M, Wall MA, Graves J, Wang Z, Ranganathan R. Dynamic scaffolding in a G protein-coupled signaling system. Cell. 2007;131:80-92.

151. Scott K, Sun Y, Beckingham K, Zuker CS. Calmodulin regulation of *Drosophila* light-activated channels and receptor function mediates termination of the light response in vivo. Cell. 1997;91:375-83.

152. Yarbus AL. Eye movements and vision. New York: Plenum; 1967.

153. Buracas GT, Albright TD. Gauging sensory representations in the brain. Trends in Neurosciences. 1999;22:303-9.

154. Farroni T, Csibra G, Simion G, Johnson MH. Eye contact detection in humans from birth. P Natl Acad Sci USA. 2002;99:9602-5.

155. Bushnell IWR. Mother's face recognition in newborn infants: Learning and memory. Infant Child Dev. 2001;10:67-74.

156. Lewkowicz DJ, Hansen-Tift AM. Infants deploy selective attention to the mouth of a talking face when learning speech. P Natl Acad Sci USA. 2012;109:1431-6.

157. Cover TM, Thomas JA. Elements of Information Theory. 2nd ed. Hoboken: John Wiley & Sons; 2005.

158. Li X, Abou Tayoun A, Song Z, Dau A, Rien D, Jaciuch D, et al. Ca^{2+}-activated K^+ channels reduce network excitability, improving adaptability and energetics for transmitting and perceiving sensory information. J Neurosci. 2019;39:7132-54.

159. Pick B. Specific Misalignments of Rhabdomere Visual Axes in Neural Superposition Eye of Dipteran Flies. Biol Cybern. 1977;26:215-24.

160. Dippé MAZ, Wold EH. Antialiasing through stochastic sampling. ACM SIGGRAPH Computer Graphics. 1985;19:69-78.

161. Yellott JI. Spectral-analysis of spatial sampling by photoreceptors - topological disorder prevents aliasing. Vis Res. 1982;22:1205-10.

162. Yellott JI. Spectral consequences of photoreceptor sampling in the rhesus retina. Science. 1983;221:382-5.

163. Galton F. *Vox populi*. Nature 1907:450-1.

164. Laughlin SB, van Steveninck RRD, Anderson JC. The metabolic cost of neural information. Nat Neurosci. 1998;1:36-41.

165. Land MF. Visual acuity in insects. Ann Rev Entomol. 1997;42:147-77.

166. MaBouDi H, Richter J, Guiraud MG, Roper M, Marshall JAR, Chittka L. Active vision of bees in a simple pattern discrimination task. Elife. 2025;14.

167. MaBouDi H, Roper M, Guiraud M, Marshall JA, Chittka L. Automated video tracking and flight analysis show how bumblebees solve a pattern discrimination task using active vision. bioRxiv. 2021.

168. Maboudi H, Roper M, Guiraud MG, Juusola M, Chittka L, Marshall JAR, et al. A neuromorphic model of active vision shows how spatiotemporal encoding in lobula neurons can aid pattern recognition in bees. Elife. 2025;14.

169. Hardie RC. Functional organization of the fly retina. Progress in Sensory Physiology: Springer; 1985. p. 1-79.

170. Srinivasan MV, Bernard GD. Effect of Motion on Visual-Acuity of Compound Eye - Theoretical-Analysis. Vision Res. 1975;15:515-25.

171. Juusola M, French AS. Visual acuity for moving objects in first- and second-order neurons of the fly compound eye. Journal of Neurophysiology. 1997;77:1487-95.

172. Riggs LA, Ratliff F. The effects of counteracting the normal movements of the eye. J Opt Soc Am. 1952;42:872-3.

173. Riggs LA, Ratliff F, Cornsweet JC, Cornsweet TN. The Disappearance of Steadily Fixated Visual Test Objects. J Opt Soc Am. 1953;43:495-501.

174. Martinez-Conde S, Macknik SL, Hubel DH. The role of fixational eye movements in visual perception. Nat Rev Neurosci. 2004;5:229-40.

175. Kahneman D. Thinking, fast and slow: Farrar, Straus and Giroux.; 2011.

176. Simoncelli EP, Olshausen BA. Natural image statistics and neural representation. Annu Rev Neurosci. 2001;24:1193-216.

177. Hubel DH, Wiesel TN. The period of susceptibility to the physiological effects of unilateral eye closure in kittens. J Physiol. 1970;206:419-36.

178. Wechsler SP, Bhandawat V. Behavioral algorithms and neural mechanisms underlying odor-modulated locomotion in insects. J Exp Biol. 2023;226.

179. Budick SA, Dickinson MH. Free-flight responses of *Drosophila melanogaster* to attractive odors. J Exp Biol. 2006;209:3001-17.

180. Stupski SD, van Breugel F. Wind gates olfaction-driven search states in free flight. Current Biology. 2024;34.

181. Lazar AA, Liu T, Yeh CH, Zhou Y. Modeling and characterization of pure and odorant mixture processing in the Drosophila mushroom body calyx. Front Physiol. 2024;15:1410946.

182. Lazar AA, Yeh CH. A molecular odorant transduction model and the complexity of spatio-temporal encoding in the antenna. Plos Comput Biol. 2020;16.

183. Behnia R, Desplan C. Visual circuits in flies: beginning to see the whole picture. Curr Opin Neurobiol. 2015;34:125-32.

184. Matsliah A, Yu SC, Kruk K, Bland D, Burke AT, Gager J, et al. Neuronal parts list and wiring diagram for a visual system. Nature. 2024;634:166-80.

185. Wachowiak M. All in a sniff: olfaction as a model for active sensing. Neuron. 2011;71:962-73.

186. Kepecs A, Uchida N, Mainen ZF. The sniff as a unit of olfactory processing. Chem Senses. 2006;31:167-79.

187. Harvey J, Rinberg D. Olfaction: Source separation in a single sniff. Curr Biol. 2021;31:R1051-R3.

188. Karadas M, Gill JV, Ceballo S, Shoham S, Rinberg D. Rapid temporal processing in the olfactory bulb underlies concentration invariant odor identification and signal decorrelation. Res Sq. 2025.

189. Shusterman R, Smear MC, Koulakov AA, Rinberg D. Precise olfactory responses tile the sniff cycle. Nat Neurosci. 2011;14:1039–44.

190. Smear M, Shusterman R, O'Connor R, Bozza T, Rinberg D. Perception of sniff phase in mouse olfaction. Nature. 2011;479:397–400.

191. Brainard DH, Wandell BA. Asymmetric Color Matching - How Color Appearance Depends on the Illuminant. Journal of the Optical Society of America a-Optics Image Science and Vision. 1992;9:1433-48.

192. Rushton WAH. Pigments and Signals in Color-Vision. J Physiol-London. 1972;220:P1-&.

193. Bandyopadhyay P, Sachse S. Mixing things up! - how odor blends are processed in Drosophila. Curr Opin Insect Sci. 2023;59:101099.

194. Blazing RM, Franks KM. Odor coding in piriform cortex: mechanistic insights into distributed coding. Curr Opin Neurobiol. 2020;64:96-102.

195. Endo K, Kazama H. Central organization of a high-dimensional odor space. Curr Opin Neurobiol. 2022;73:102528.

196. Intoy J, Rucci M. Finely tuned eye movements enhance visual acuity. Nat Commun. 2020;11.

197. Rucci M, Ahissar E, Burr D. Temporal Coding of Visual Space. Trends Cogn Sci. 2018;22:883-95.

198. Pisokas I, Heinze S, Webb B. The head direction circuit of two insect species. Elife. 2020;9.

199. Seelig JD, Jayaraman V. Feature detection and orientation tuning in the *Drosophila* central complex. Nature. 2013;503:262-6.

200. Cope AJ, Sabo C, Vasilaki E, Barron AB, Marshall JAR. A computational model of the integration of landmarks and motion in the insect central complex. Plos One. 2017;12.

201. Dan C, Hulse BK, Kappagantula R, Jayaraman V, Hermundstad AM. A neural circuit architecture for rapid learning in goal-directed navigation. Neuron. 2024;112:2581-99 e23.

202. Garner D, Kind E, Lai JYH, Nern A, Zhao A, Houghton L, et al. Connectomic reconstruction predicts visual features used for navigation. Nature. 2024;634:181-90.

203. Goulard R, Buehlmann C, Niven JE, Graham P, Webb B. A unified mechanism for innate and learned visual landmark guidance in the insect central complex. Plos Comput Biol. 2021;17:e1009383.

204. Grabowska MJ, Jeans R, Steeves J, van Swinderen B. Oscillations in the central brain of Drosophila are phase locked to attended visual features. Proc Natl Acad Sci U S A. 2020;117:29925-36.

205. Green J, Adachi A, Shah KK, Hirokawa JD, Magani PS, Maimon G. A neural circuit architecture for angular integration in *Drosophila*. Nature. 2017;546:101-6.

206. Heinze S. Mapping the fly's 'brain in the brain'. Elife. 2021;10.

207. Heinze S, Homberg U. Linking the input to the output: new sets of neurons complement the polarization vision network in the locust central complex. J Neurosci. 2009;29:4911-21.

208. Hulse BK, Haberkern H, Franconville R, Turner-Evans D, Takemura SY, Wolff T, et al. A connectome of the *Drosophila* central complex reveals network motifs suitable for flexible navigation and context-dependent action selection. Elife. 2021;10.

209. Li F, Lindsey J, Marin EC, Otto N, Dreher M, Dempsey G, et al. The connectome of the adult mushroom body provides insights into function. Elife. 2020;9.

210. Pfeiffer K, Homberg U. Organization and functional roles of the central complex in the insect brain. Annu Rev Entomol. 2014;59:165-U787.

211. Eichler K, Li F, Litwin-Kumar A, Park Y, Andrade I, Chneider-Mizell CMS, et al. The complete connectome of a learning and memory centre in an insect brain. Nature. 2017;548:175-82.

212. MaBouDi H, Marshall JAR, Barron AB. Honeybees solve a multi-comparison ranking task by probability matching. P Roy Soc B-Biol Sci. 2020;287.

213. Nityananda V, Chittka L. Modality-specific attention in foraging bumblebees. Roy Soc Open Sci. 2015;2.

214. Sorribes A, Armendariz BG, Lopez-Pigozzi D, Murga C, de Polavieja GG. The origin of behavioral bursts in decision-making circuitry. Plos Comput Biol. 2011;7:e1002075.

215. Takemura SY, Aso Y, Hige T, Wong A, Lu Z, Xu CS, et al. A connectome of a learning and memory center in the adult Drosophila brain. Elife. 2017;6.

216. Mostofi N, Zhao Z, Intoy J, Boi M, Victor JD, Rucci M. Spatiotemporal Content of Saccade Transients. Curr Biol. 2020;30:3999-4008 e2.

217. Barlow HB. Eye movements during fixation. J Physiol. 1952;116:290-306.

218. Ahissar E, Arieli A. Seeing via Miniature Eye Movements: A Dynamic Hypothesis for Vision. Front Comput Neurosci. 2012;6:89.

219. Aytekin M, Victor JD, Rucci M. The visual input to the retina during natural head-free fixation. J Neurosci. 2014;34:12701-15.

220. Rucci M, Poletti M. Control and Functions of Fixational Eye Movements. Annual Review of Vision Science, Vol 1. 2015;1:499-518.

221. Zhao Z, Ahissar E, Victor JD, Rucci M. Inferring visual space from ultra-fine extra-retinal knowledge of gaze position. Nat Commun. 2023;14:269.

222. Kern R, van Hateren JH, Michaelis C, Lindemann JP, Egelhaaf M. Function of a fly motion-sensitive neuron matches eye movements during free flight. PLoS Biol. 2005;3:e171.

223. Field DJ. Relations between the statistics of natural images and the response properties of cortical cells. J Opt Soc Am A. 1987;4:2379-94.

224. Martinez-Conde S, Otero-Millan J, Macknik SL. The impact of microsaccades on vision: towards a unified theory of saccadic function. Nat Rev Neurosci. 2013;14:83-96.

225. Noton D, Stark L. Scanpaths in Saccadic Eye Movements While Viewing and Recognizing Patterns. Vision Res. 1971;11:929-&.

226. Noton D, Stark L. Scanpaths in Eye Movements during Pattern Perception. Science. 1971;171:308-&.

227. Najemnik J, Geisler WS. Optimal eye movement strategies in visual search. Nature. 2005;434:387-91.

228. Rothkopf CA, Ballard DH, Hayhoe MM. Task and context determine where you look. J Vision. 2007;7.

229. Guiraud M, Roper M, Chittka L. High-Speed Videography Reveals How Honeybees Can Turn a Spatial Concept Learning Task Into a Simple Discrimination Task by Stereotyped Flight Movements and Sequential Inspection of Pattern Elements. Front Psychol. 2018;9.

230. Land MF, Collett TS. Chasing Behavior of Houseflies (Fannia-Canicularis) - Description and Analysis. J Comp Physiol. 1974;89:331-57.

231. Boeddeker N, Kern R, Egelhaaf M. Chasing a dummy target: smooth pursuit and velocity control in male blowflies. P Roy Soc B-Biol Sci. 2003;270:393-9.

232. Atick JJ, Redlich AN. What Does the Retina Know About Natural Scenes. Neural Computation. 1992;4:196-210.

233. Olshausen BA. Learning sparse, overcomplete representations of time-varying natural images. Ieee Image Proc. 2003;41-4.

234. MaBouDi H, Marshall JAR, Dearden N, Barron AB. How honey bees make fast and accurate decisions. BioRxiv. 2023.

235. Gold JI, Shadlen MN. The neural basis of decision making. Annual Review of Neuroscience. 2007;30:535-74.

236. Heitz RP, Schall JD. Neural Mechanisms of Speed-Accuracy Tradeoff. Neuron. 2012;76:616-28.

237. Hanks TD, Kiani R, Shadlen MN. A neural mechanism of speed-accuracy tradeoff in macaque area LIP. Elife. 2014;3.

238. Bogacz R. Optimal decision-making theories: linking neurobiology with behaviour. Trends in Cognitive Sciences. 2007;11:118-25.

239. Chittka L, Skorupski P, Raine NE. Speed-accuracy tradeoffs in animal decision making. Trends Ecol Evol. 2009;24:400-7.

240. Marshall JAR, Dornhaus A, Franks NR, Kovacs T. Noise, cost and speed-accuracy trade-offs: decision-making in a decentralized system. J R Soc Interface. 2006;3:243-54.

241. Ruderman DL, Cronin TW, Chiao CC. Statistics of cone responses to natural images: implications for visual coding. Journal of the Optical Society of America a-Optics Image Science and Vision. 1998;15:2036-45.

242. Geurten BRH, Jahde P, Corthals K, Gopfert MC. Saccadic body turns in walking *Drosophila*. Front Behav Neurosci. 2014;8.

243. von Frisch K. The dance language and orientation of bees. Cambridge: Harvard University Press; 1967.

244. Seeley TD. The Wisdom of the Hive: The Social Physiology of Honey Bee Colonies. Cambridge: Harvard University Press; 1995.

245. Hadjitofi A, Webb B. Dynamic antennal positioning allows honeybee followers to decode the dance. Curr Biol. 2024;34:1772-9 e4.

246. Pavlou HJ, Goodwin SF. Courtship behavior in Drosophila melanogaster: towards a 'courtship connectome'. Curr Opin Neurobiol. 2013;23:76-83.

247. Coen P, Murthy M. Singing on the fly: sensorimotor integration and acoustic communication in Drosophila. Curr Opin Neurobiol. 2016;38:38-45.

248. Levy WB, Baxter RA. Energy efficient neural codes. Neural Computation. 1996;8:531-43.

249. Attwell D, Laughlin SB. An energy budget for signaling in the grey matter of the brain. J Cerebr Blood F Met. 2001;21:1133-45.

250. Ma WJ, Beck JM, Latham PE, Pouget A. Bayesian inference with probabilistic population codes. Nat Neurosci. 2006;9:1432-8.

251. Zhang WH, Wu S, Josic K, Doiron B. Sampling-based Bayesian inference in recurrent circuits of stochastic spiking neurons. Nat Commun. 2023;14:7074.

252. Knill DC, Pouget A. The Bayesian brain: the role of uncertainty in neural coding and computation. Trends Neurosci. 2004;27:712-9.

253. Schultz W, Dayan P, Montague PR. A neural substrate of prediction and reward. Science. 1997;275:1593-9.

254. Lanore F, Cayco-Gajic NA, Gurnani H, Coyle D, Silver RA. Cerebellar granule cell axons support high-dimensional representations. Nat Neurosci. 2021;24:1142-50.

255. Silver RA, Lubke J, Sakmann B, Feldmeyer D. High-probability uniquantal transmission at excitatory synapses in barrel cortex. Science. 2003;302:1981-4.

256. Alle H, Geiger JR. Combined analog and action potential coding in hippocampal mossy fibers. Science. 2006;311:1290-3.

257. de Polavieja GG, Harsch A, Kleppe I, Robinson HP, Juusola M. Stimulus history reliably shapes action potential waveforms of cortical neurons. J Neurosci. 2005;25:5657-65.

258. Juusola M, Robinson HP, de Polavieja GG. Coding with spike shapes and graded potentials in cortical networks. Bioessays. 2007;29:178-87.

259. Shu Y, Hasenstaub A, Duque A, Yu Y, McCormick DA. Modulation of intracortical synaptic potentials by presynaptic somatic membrane potential. Nature. 2006;441:761-5.

260. de Kock CPJ, Feldmeyer D. Shared and divergent principles of synaptic transmission between cortical excitatory neurons in rodent and human brain. Front Synaptic Neuro. 2023;15.

261. Eyal G, Verhoog MB, Testa-Silva G, Deitcher Y, Benavides-Piccione R, DeFelipe J, et al. Human Cortical Pyramidal Neurons: From Spines to Spikes via Models. Front Cell Neurosci. 2018;12.

262. Leleo EG, Segev I. Burst control: Synaptic conditions for burst generation in cortical layer 5 pyramidal neurons. Plos Comput Biol. 2021;17.

263. Laughlin SB, Sejnowski TJ. Communication in neuronal networks. Science. 2003;301:1870-4.

264. Pillow JW, Shlens J, Paninski L, Sher A, Litke AM, Chichilnisky EJ, et al. Spatio-temporal correlations and visual signalling in a complete neuronal population. Nature. 2008;454:995-9.
265. Juusola M, French AS. The efficiency of sensory information coding by mechanoreceptor neurons. Neuron. 1997;18:959-68.
266. Mainen ZF, Sejnowski TJ. Reliability of Spike Timing in Neocortical Neurons. Science. 1995;268:1503-6.
267. Boyden ES, Zhang F, Bamberg E, Nagel G, Deisseroth K. Millisecond-timescale, genetically targeted optical control of neural activity. Nat Neurosci. 2005;8:1263-8.

Disclaimer/Publisher's Note: The statements, opinions and data contained in all publications are solely those of the individual author(s) and contributor(s) and not of MDPI and/or the editor(s). MDPI and/or the editor(s) disclaim responsibility for any injury to people or property resulting from any ideas, methods, instructions or products referred to in the content.